

2

**AD-A252 279**



**Technical Document 2271**  
**June 1992**

**An Evaluation of an  
Infrared/Resistance  
Temperature Device  
for Air/Sea-Surface  
Temperature  
Measurements**

W. L. Patterson



**92-17115**



92 6 29 107

Approved for public release; distribution is unlimited.



**NAVAL COMMAND, CONTROL AND  
OCEAN SURVEILLANCE CENTER  
RDT&E DIVISION  
San Diego, California 92152-5000**

**J. D. FONTANA, CAPT, USN**  
Commanding Officer

**R. T. SHEARER**  
Executive Director

**ADMINISTRATIVE INFORMATION**

This work was performed for the Space and Naval Warfare Systems Command (PMW-165), Washington, DC 20363-5100, under project X2008. The work was funded under program element 0603207N and was performed by members of the Tropospheric Branch, Code 543, Naval Command, Control and Ocean Surveillance Center, RDT&E Division, San Diego, California 92152-5000.

Released by  
R. A. Paulus, Head  
Tropospheric Branch

Under authority of  
J. H. Richter, Head  
Ocean and Atmospheric  
Sciences Division

<b>Accession For</b>	
NTIS GRA&I	<input checked="" type="checkbox"/>
DTIC TAB	<input type="checkbox"/>
Unannounced	<input type="checkbox"/>
Justification	
By	
Distribution/	
Availability Codes	
Dist	Avail and/or Special
A-1	

MA

# CONTENTS

BACKGROUND .....	1
AIR AND SEA-SURFACE TEMPERATURES .....	1
EVAPORATION DUCTS .....	3
EXPERIMENTAL TECHNIQUE .....	4
RESULTS .....	5
DEVICE RELIABILITY .....	5
OTHER DEVICE USES .....	5
AIR AND SEA-SURFACE TEMPERATURE DATA .....	6
EVAPORATION DUCT CALCULATIONS .....	10
CONCLUSIONS AND RECOMMENDATIONS .....	17
REFERENCES .....	19
APPENDIX A: AIR AND SEA-SURFACE TEMPERATURES, AIR/SEA- SURFACE TEMPERATURE DIFFERENCES, AND COMPUTED EVAPORATION DUCT HEIGHTS, 12-24 JULY 1991 .....	A-1

## FIGURES

1. Annual air/sea-temperature difference distribution from NOAA ocean buoy 42002 .....	2
2. Annual air/sea-surface temperature difference distribution from Marsden square 82 .....	3
3. Evaporation duct height distribution .....	4
4. Air temperature differences (°F) as measured with a hand-held electric psychrometer and the IR/RTD .....	7
5. Sea-surface temperature differences (°F) as measured by seawater intake gauge and the IR/RTD .....	7
6. Air/sea temperature differences (°F) (psychrometer/engineering intake gauge) .....	8
7. Air/sea temperature differences (°F) (IR/RTD) .....	9
8. Sea-surface temperatures (°F) of 17 July 1991 .....	10

## CONTENTS (continued)

9. Evaporation duct height distribution. No stability correction applied .....	11
10. Evaporation duct height distribution. Stability correction applied .....	12
11. Evaporation duct height (m) differences .....	13
12. Modified refractive index versus height profiles for 0300 GMT, 13 July 1991. (Psychrometer/engine and IR/RTD sensors.) .....	14
13. 3-GHz propagation loss within a 4.7- and 6.2-meter evaporation ducting environment .....	15
14. 9.6-GHz propagation loss within a 4.7- and 6.2-meter evaporation ducting environment .....	16
15. 15-GHz propagation loss within a 4.7- and 6.2-meter evaporation ducting environment .....	16
16. Measured signal strengths about mean signal strength predictions for various propagation models (Dockery, 1987) .....	17

## BACKGROUND

The air in contact with the ocean's surface is saturated with water vapor. A few meters above the surface, the air is not usually saturated so there is a decrease in water vapor pressure from the surface to some value well above the surface. This decrease in water vapor pressure leads to a decrease in the refractive index of the air that forms an "evaporation" duct, a channel in which electromagnetic (EM) energy can propagate over great ranges, significantly influencing radio and radar transmissions (Hitney, et al., 1987).

Evaporation ducts exist over the ocean, to some degree, almost all of the time. The height varies from 1 or 2 meters in northern latitudes during winter nights to as much as 40 meters in equatorial latitudes during summer days. It should be emphasized that the evaporation duct "height" is not a height below which an antenna must be located to have extended propagation, but a value that relates to the duct's strength or its ability to trap EM radiation.

Evaporation duct heights may be calculated by measuring wind speed, sea-surface temperature, air temperature, and relative humidity. A critical component of the calculation is the relative difference between air and sea-surface temperatures. This technical report examines results from an at-sea test of a noncontact infrared, resistance temperature device (IR/RTD) for use in measuring the air/sea-surface temperature differences.

## AIR AND SEA-SURFACE TEMPERATURES

In the absence of warm temperature advection, the marine surface layer is slightly unstable due to the different heat capacities of air and water. In other words, the air temperature is slightly cooler than the sea-surface temperature. This unstable condition is by far the most common situation over open ocean areas. This unstable condition may be seen in figure 1, that illustrates the annual air/sea-surface temperature difference distribution from the National Oceanic and Atmospheric Administration (NOAA) ocean buoy 42022 located at latitude 32.3 north, longitude 75.2 west (Paulus, 1984).

The elements of air and sea-surface temperature measured by transiting ships have been, for the most part, sufficiently accurate for general meteorological and climatological purposes. Measurement errors in air and sea-surface temperatures are made however, and these errors may occur in a number of ways. For example, air temperatures reported by ships in the tropics appear to be consistently high under sunny conditions due to poor instrument exposure and heat radiation from adjacent metal surfaces.

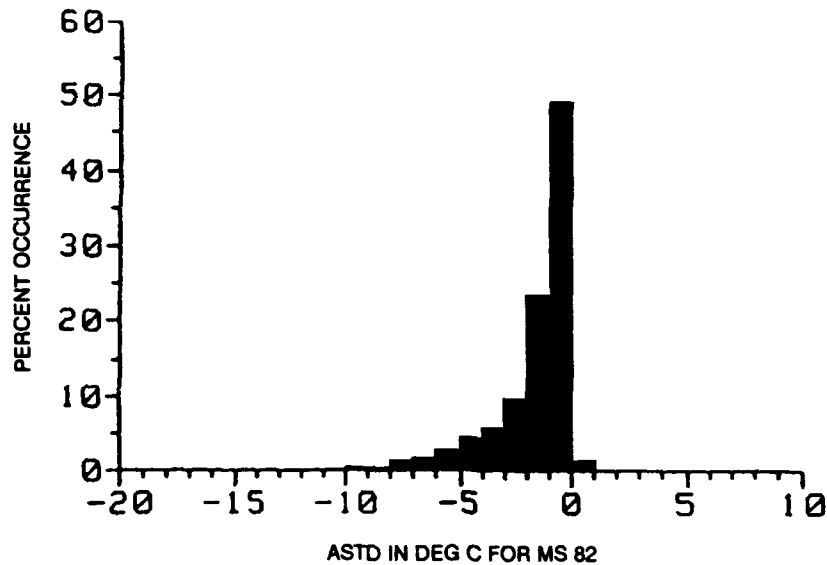


Figure 1. Annual air/sea-temperature difference distribution from NOAA ocean buoy 42002.

Sea-surface temperatures have typically been determined by measuring the seawater intake for engine cooling with readings taken by engine-room personnel from analog gauges located in the powerplant spaces. Calibration and reading errors are common. These water inlets do not measure surface temperature because they are located well below the surface and are also subject to thermal contamination.

Compounding the problem of air and sea-surface temperature differences is the fact that air and sea-surface temperature measurements are made using two different sensors that are most likely not calibrated together.

The errors in measurements produce an air/sea-surface temperature difference distribution such as illustrated in figure 2 (Paulus, 1984). Figure 2 was constructed from over 100 years of shipboard meteorological measurements from within Marsden square 82, a 10 degree latitude by 10 degree longitude square containing NOAA buoy 42002. By comparing figure 1 with figure 2, a bias toward stable, anomalous conditions by shipboard measurements is evident.

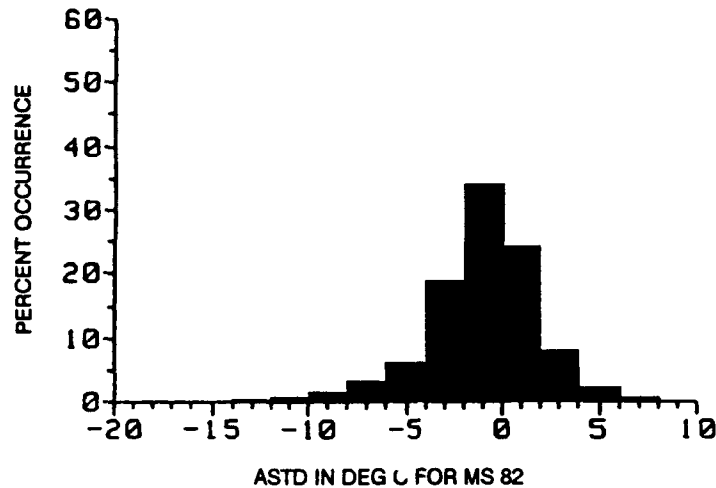


Figure 2. Annual air/sea-temperature difference distribution from Marsden square 82.

## EVAPORATION DUCTS

A critical component of the calculation of evaporation duct height is the relative difference between air and sea-surface temperatures, therefore any errors in temperature measurements could be reflected in the evaporation duct height.

For example, figure 3 illustrates the evaporation duct height distribution calculated from shipboard measurements of air/sea-surface temperature differences as shown in figure 2. Of particular note is the large occurrence of evaporation duct heights in excess of 40 meters, which in turn leads to overly optimistic propagation ranges. Since such a distribution of duct heights in nature would be extremely suspect, the accuracy of measurements used for evaporation duct calculations may not be sufficient.

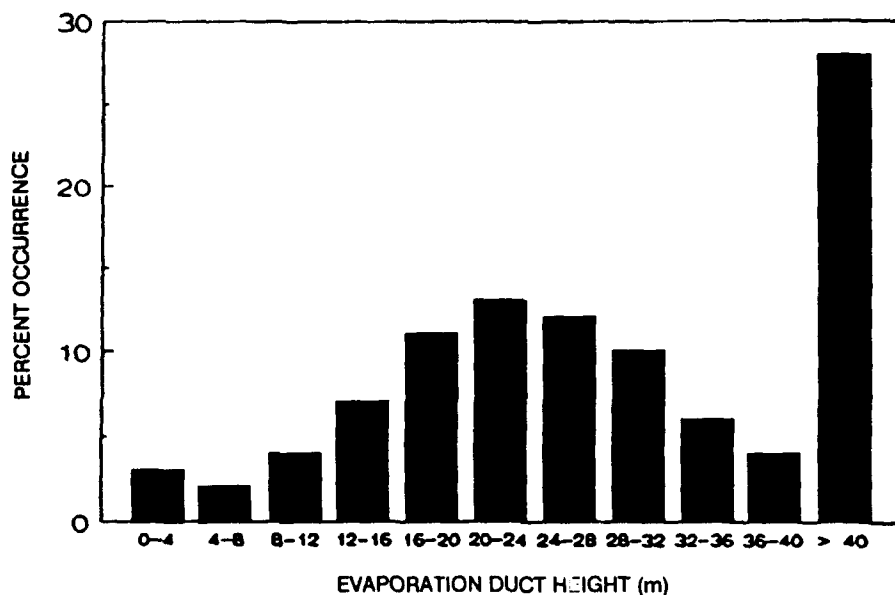


Figure 3. Evaporation duct height distribution.

## EXPERIMENTAL TECHNIQUE

As a possible solution to overcoming air and sea-surface temperature measurement errors, Olson (1989) describes an IR/RTD system manufactured by Everest Interscience, Inc., that is small, easy, and quick to use. Since Olson has demonstrated the device's measurement accuracy, he recommended further tests to evaluate the practicality of using the IR/RTD and determine acceptable shipboard environmental operating conditions.

To this end, two IR/RTD systems were purchased and placed onboard the *USS Ranger* (CV 61) for a 12-day at-sea period, from 12 to 24 July 1991. Instructions in the system's proper use and maintenance were provided as described by Olson, but no undue emphasis was placed on special handling beyond that for any hand-held electronic instrument.

While certain "best observation locations" for air and sea-surface temperature measurements were suggested by Olson, their use may not be practical on an operational ship because of the safety restrictions of movement during flight operations. For this reason, only general observation location guidelines were given, e.g., avoid locations adjacent to engineering air discharge vents.

Hourly observations were made from three locations: (a) the 09 level forward air defense station, a normal meteorological observation point during flight operations and under simulated battle conditions; (b) the flight deck; (c) and the hangar bay. The meteorological observers recorded hourly readings of air temperature from both the IR/RTD and a hand-held psychrometer, sea-surface temperatures obtained from the IR/RTD, and



seawater injection temperature reported by the engineering watch officer. In addition, measurements of surface wind speed, wind direction, and relative humidity were recorded for use in evaporation duct height calculations.

## **RESULTS**

### **DEVICE RELIABILITY**

On 13 July, one device ceased to operate while in use at the forward air defense station. The sea-surface temperature indicator showed a constant 90.4°F and the air temperature indicator showed a rapid and continuous increase. It should be noted that the SPS-48 radar is located just above this position and two UHF transmitting antennas are located on either side of the 09 level position. While it was not known if the three radio-frequency (RF) sources damaged the IR/RTD electronics, the 09 level was abandoned as a test site for the remainder of the test period. This device remained inoperative.

The IR/RTD air temperature was measured with a small gold-foil-covered thermistor located at the end of a short rod, which is pulled from the housing. After one days' use, the observer was no longer able to pull the rod to its full extent from the housing nor was he able to push it back into the housing. The lack of full-rod extension, however, appeared to have no effect on the temperature measurements.

The device is provided with a wrist strap that is attached to the handle with a plastic swivel. On July 17, the wrist strap mysteriously disappeared. Without the wrist strap, the observer had to hold the device at all times, thereby preventing the use of his hand for other purposes. The wrist strap from the inoperative device was substituted for the remainder of the test period.

The device liquid crystal display (LCD) was not back-lit for nighttime use. The observer therefore had to carry a flashlight. These two items, plus the hand-held psychrometer and on occasion, a sound-powered telephone set, made using the shipboard ladders extremely challenging. It should be noted that the IR temperature can be stored in the device's memory and retrieved and displayed at a later time. The air temperature cannot be stored in the device's memory.

### **OTHER DEVICE USES**

While this test was to determine the practicality of the IR/RTD for use in evaporation duct calculations, two other uses were identified by the meteorological personnel.

A major forecasting parameter for flight operations is the time fog will dissipate. The forecast time is highly dependent upon the stability of the air that in turn, depends upon

the temperature of the sea-surface. It was noticed that on many occasions, the forecast time lagged the actual dissipation time. Using the IR/RTD for sea-surface temperature measurements, "warm tongues" of surface water were identified that were not evident from the seawater intake temperature. Knowledge of these warm tongues significantly improved the forecast for fog dissipation.

Overheating of vital electronic equipment is always a concern for operational personnel. During the test period, an engineering failure resulted in a loss of air conditioning to the meteorological spaces housing the Tactical Environmental Support System (TESS) computers. The IR/RTD was used to sense the temperature of the computer cabinets, allowing the operators to safely turn off the computers when the maximum operating temperature was reached.

#### AIR AND SEA-SURFACE TEMPERATURE DATA

Figure 4 illustrates the difference between the air temperatures measured with the hand-held psychrometer and the air temperatures measured by the IR/RTD over the test period. While in the mean, the difference was  $0.5^{\circ}\text{F.}$ , individual differences range from  $-4.7^{\circ}$  to  $+8.8^{\circ}\text{F.}$  Although not known at this time, one explanation for the extremes in temperature difference could be due to the difficulty of reading a liquid-in-glass thermometer vice a digital display. Interestingly the hand-held psychrometer tended to record higher air temperatures than the IR/RTD. This is consistent with the historically higher air temperatures discussed in the section on air and sea-surface temperatures.

Figure 5 illustrates the difference between seawater temperatures measured from the engineering seawater intake and the sea-surface temperatures measured by the IR/RTD over the test period. In the mean, the temperature difference was  $0.6^{\circ}\text{F.}$ , that on first impression was quite good, but individual differences range from  $-6.0^{\circ}$  to  $+11.0^{\circ}\text{F.}$  As with the air temperature, the seawater intake temperature was almost universally warmer than that measured by the IR/RTD. This was expected due to thermal contamination in the engineering spaces. In addition, because the atmosphere is generally unstable, there is a greater heat loss from the surface water to the air than that occurring at depth from mixing within the water column.

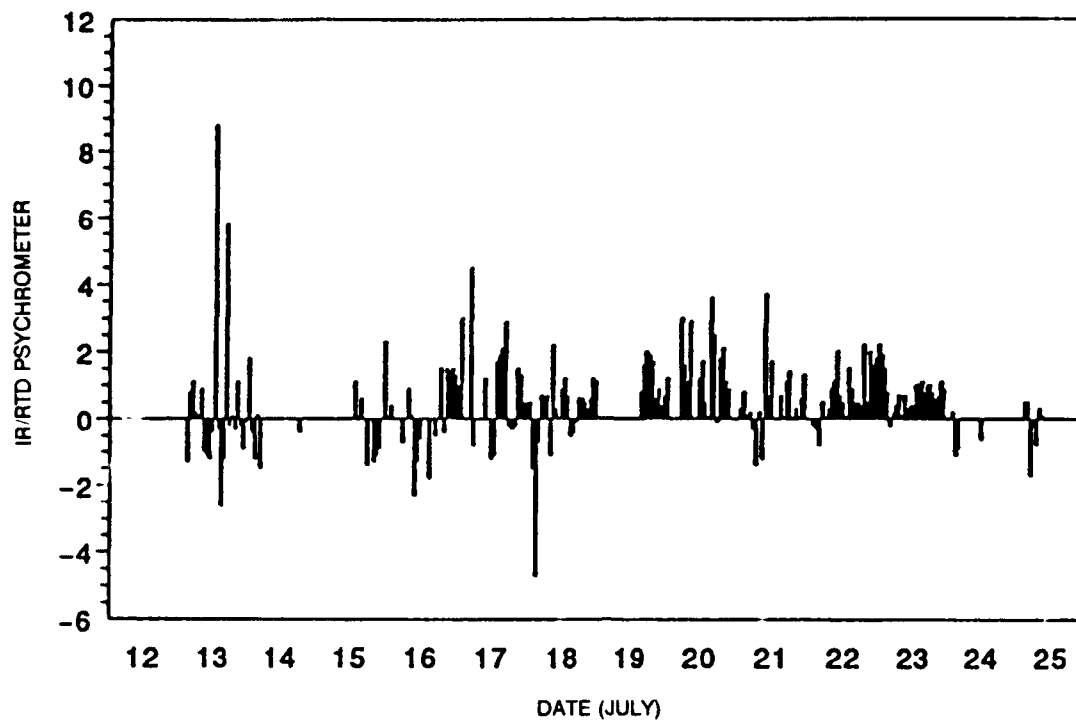


Figure 4. Air temperature differences ( $^{\circ}\text{F}$ ) as measured with a hand-held electric psychrometer and the IR/RTD.

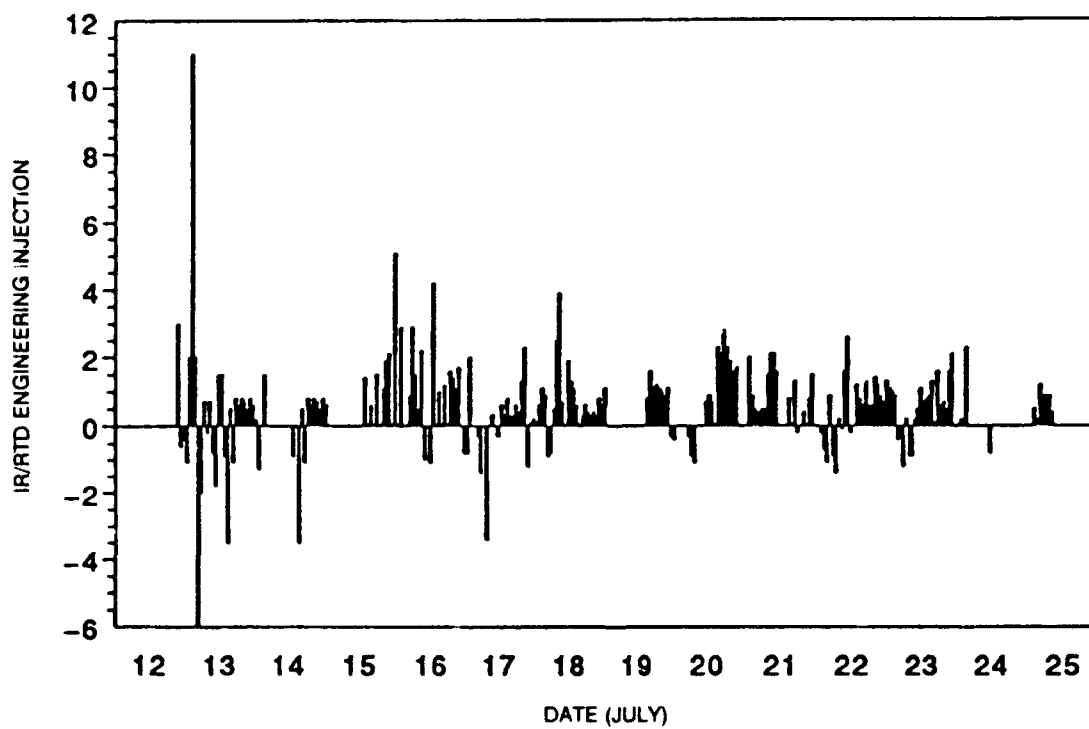


Figure 5. Sea-surface temperature differences ( $^{\circ}\text{F}$ ) as measured by seawater intake gauge and the IR/RTD.

Figure 6 illustrates the air/sea-surface temperature differences calculated from the hand-held psychrometer/seawater intake gauge. In the mean, the temperature difference was  $-1.09^{\circ}\text{F}$  with individual differences ranging from  $-5^{\circ}\text{F}$  to  $+5^{\circ}\text{F}$ . For the most part, slightly unstable conditions were observed throughout the time period with stable conditions appearing in the mid to late afternoons.

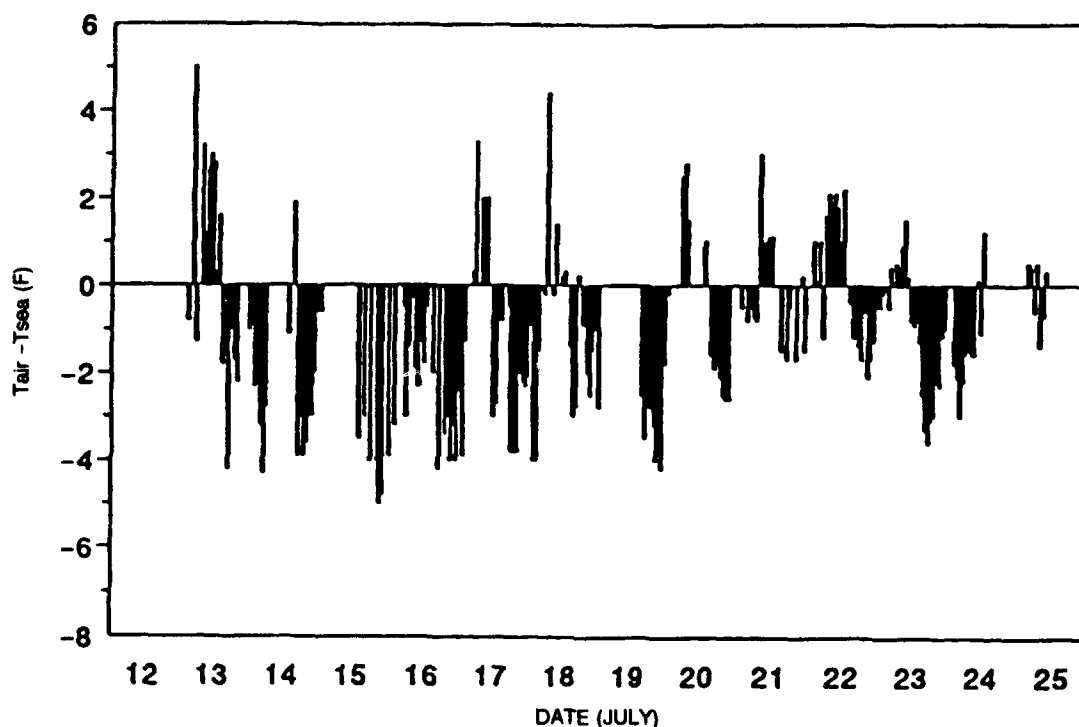


Figure 6. Air/sea temperature differences ( $^{\circ}\text{F}$ ) (psychrometer/engineering intake gauge).

Figure 7 illustrates the air/sea-surface temperature differences calculated from the IR/RTD. In the mean, the temperature difference was  $-0.96^{\circ}\text{F}$  with individual differences ranging from  $-8^{\circ}\text{F}$  to  $+4.5^{\circ}\text{F}$ .

Good agreement between the two measurement systems suggested the atmosphere was typically unstable. Measurements from both systems indicated an increase in stability toward the early- and mid-afternoon hours. This apparent stability increase may have been due to the air temperature measurements being contaminated by the heat island effects of the ship.

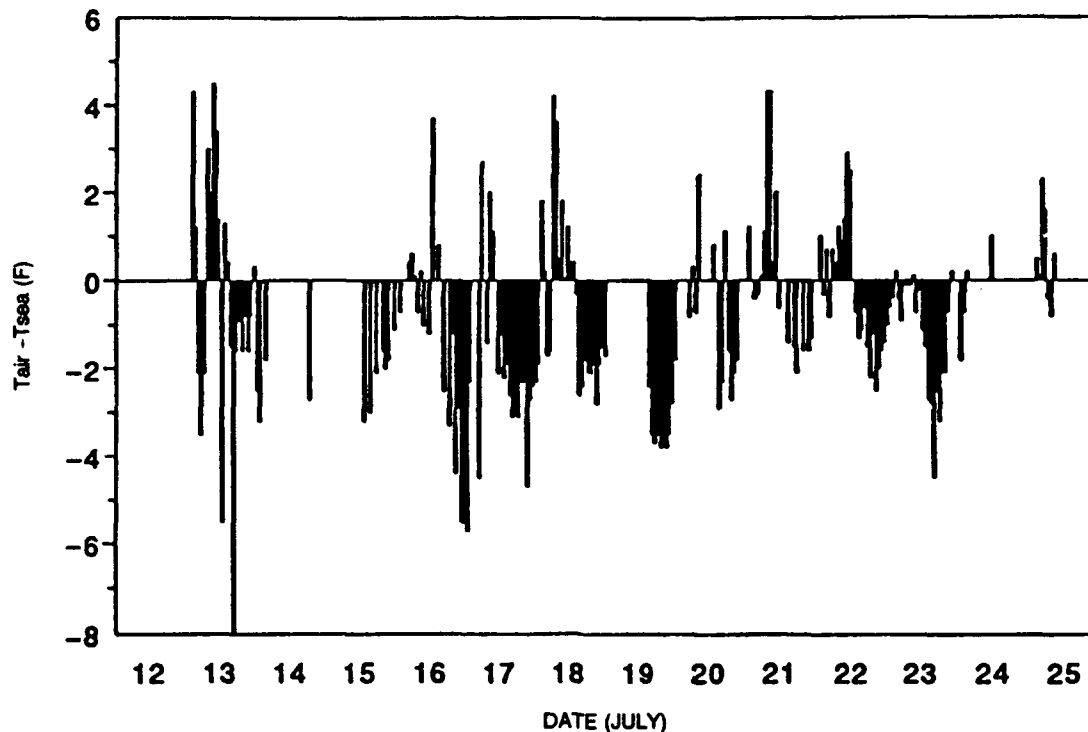


Figure 7. Air/sea temperature differences (°F) (IR/RTD).

The figures in appendix A illustrate the day-by-day air temperatures, sea-surface temperatures, and air/sea-surface temperature differences as measured by the two systems; and the computed evaporation duct heights.

Of particular note was the seawater temperature as measured by the engineering gauge. Often times the water temperature remained constant for several hours, changed sharply, and then returned to a constant value. Figure 8 is a particularly striking example. The temperature changes occurred on the hours that engineering personnel change shifts, with the temperature remaining constant for the normal four-hour watch period. Since this temperature pattern was not seen by the IR/RTD temperature readings, the ability of the seawater intake temperature to represent an actual sea-surface temperature was questionable. Given this artificiality, however, it was surprising to see the close agreement between the air/sea-surface temperature differences between the two systems. It appeared that, for at least this measurement period, air/sea-surface temperature differences measured using the engineering intake and the psychrometer did indeed represented good measurements.

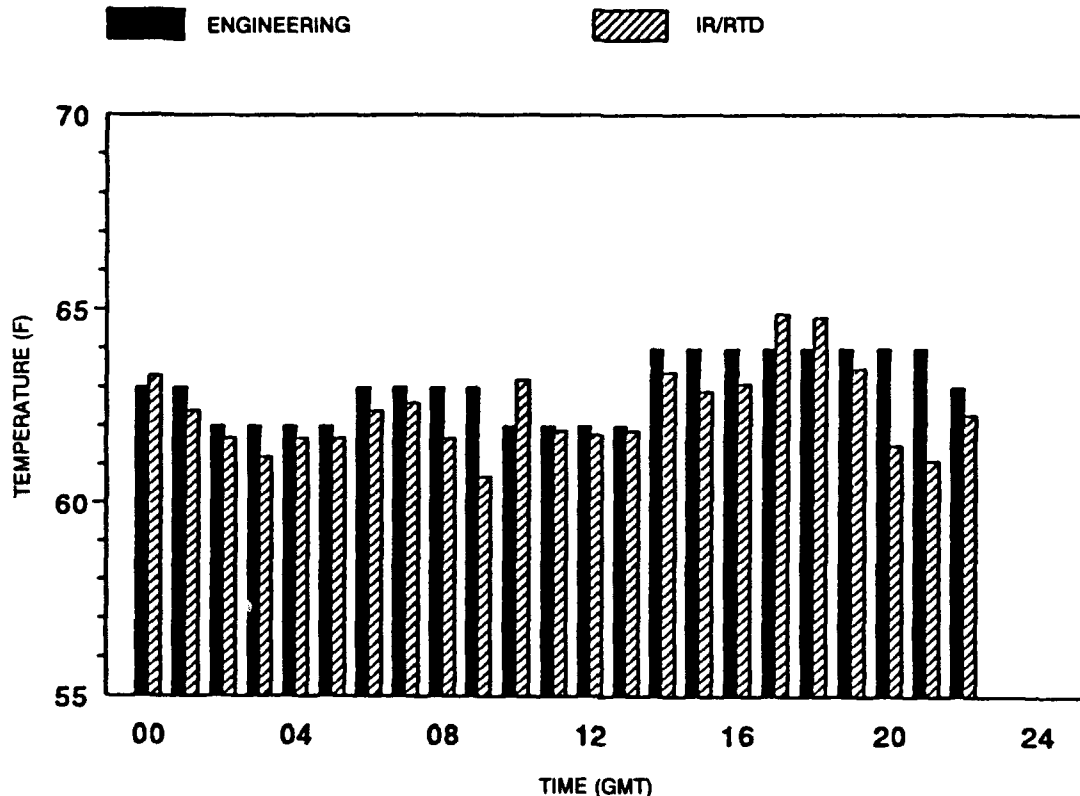


Figure 8. Sea-surface temperatures (°F) of 17 July 1991.

## EVAPORATION DUCT CALCULATIONS

To compensate for observational errors that produce this anomalous evaporation duct heights (figure 3), Paulus (1984) introduced a modification to the evaporation duct height calculation algorithm that restores the normal open-ocean unstable atmospheric conditions. Figure 9 illustrates the distribution of evaporation duct heights calculated from the observed data of both measurement systems without applying the stability compensation technique. Comparing figures 9 and 3, the same trend of abnormally high occurrence of evaporation duct heights equal to or exceeding 40 meters is quite evident.

Recalculating the evaporation duct heights with the Paulus stability modification produces a distribution illustrated in figure 10. A distribution of duct heights is obtained that agrees with the long-term climatological distribution of duct heights for the area and time period (Patterson, 1987).

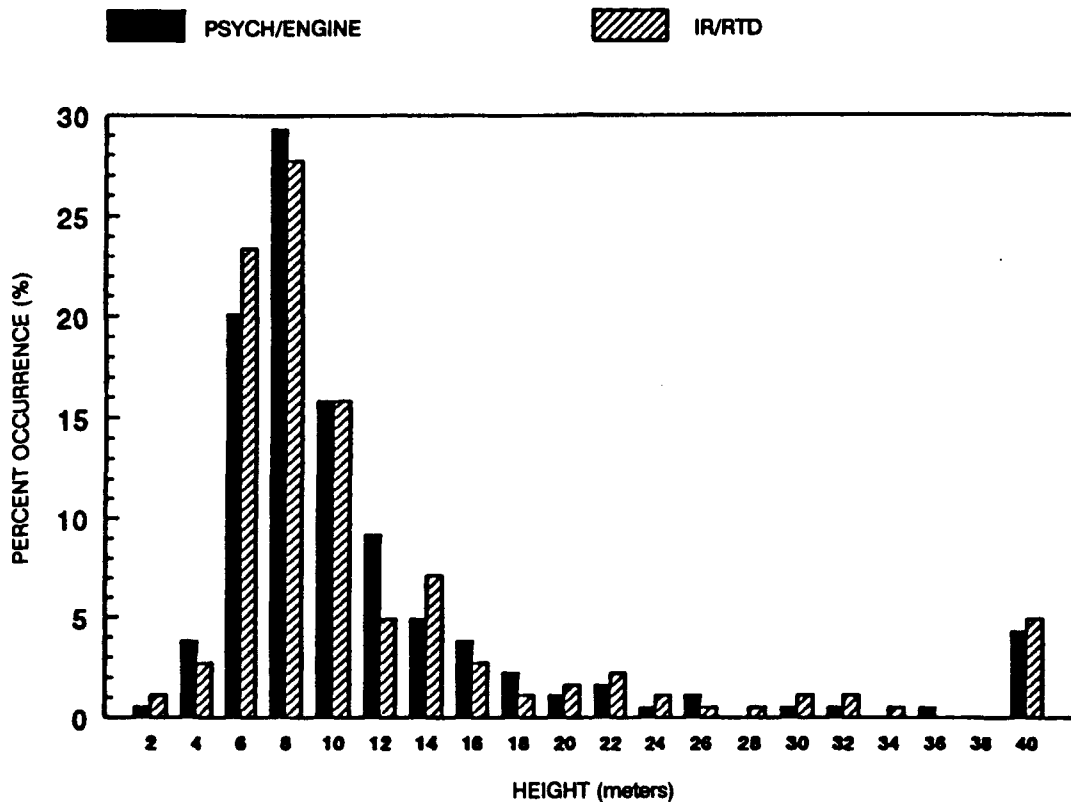


Figure 9. Evaporation duct height distribution. No stability correction applied.

Patterson (1984) has shown that while most commonly used evaporation duct height models perform equally well under statistically averaged meteorological parameters, individual evaporation duct height calculations are extremely dependent on individual meteorological parameters. Therefore, while the statistical mean of the two measurement systems examined appear to be consistent, the fluctuations in extremes are of major concern. Any measurement errors introduced are equally of concern.

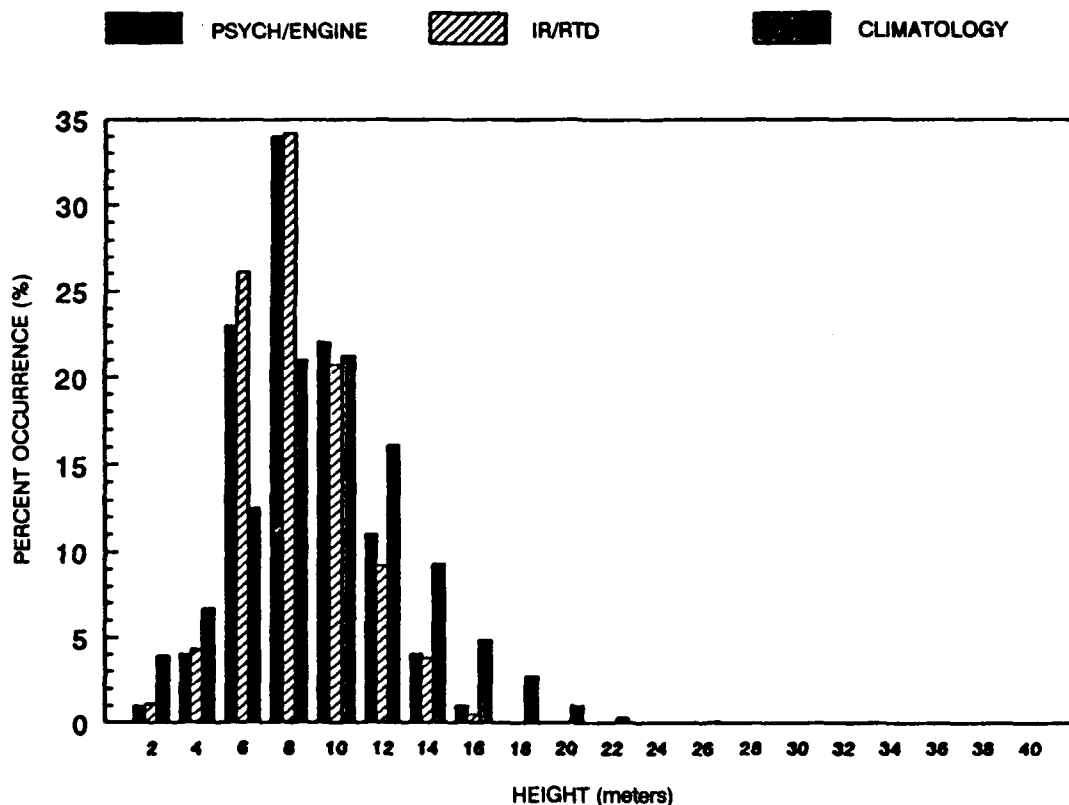


Figure 10. Evaporation duct height distribution. Stability correction applied.

Figure 11 illustrates the evaporation duct height differences as calculated from the temperature measurements provided by the two systems. Again, the Paulus stability modification was applied to the duct height calculations. The mean duct height differences over the 12-day time period were less than 1 meter with extremes of 2 meters or less. A further investigation of surface pressures, wind directions, and relative humidities during this period indicates the entire time period was spent under the influence of a single maritime air mass. Therefore, it is realistic to observe differences between the measured evaporation duct height distribution and climatology.



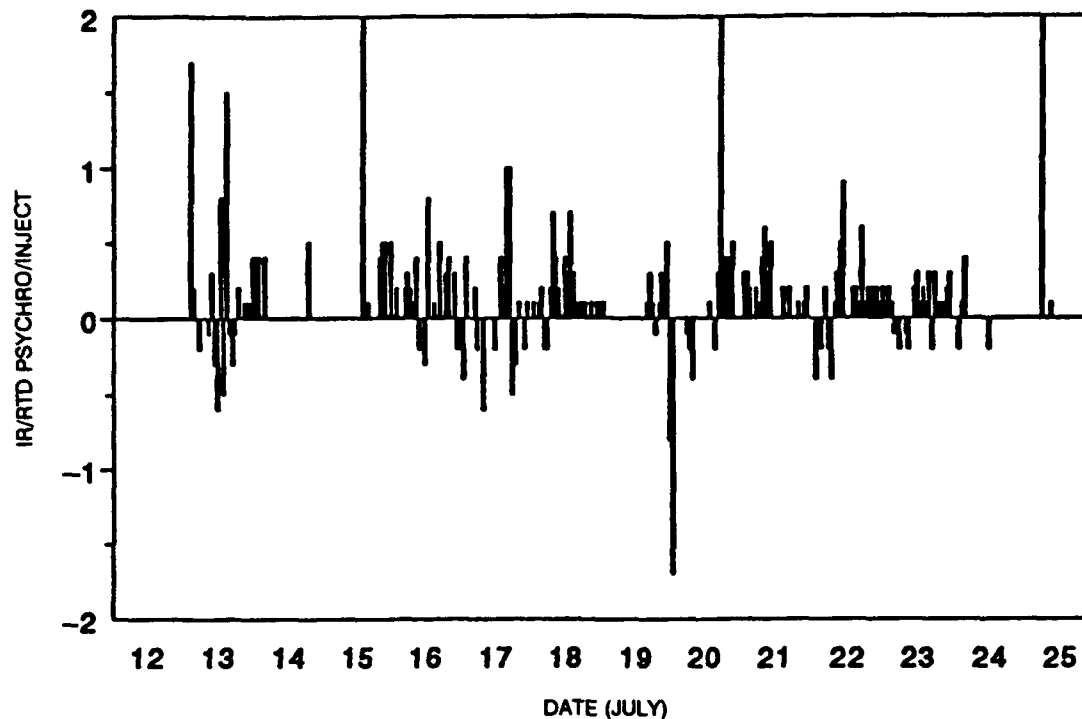


Figure 11. Evaporation duct height (m) differences.

While accurate evaporation duct height calculations are the goal of any temperature measurement system, the influence of the evaporation duct upon EM propagation is the ultimate criterion for judging a successful system. In current operational propagation models, the evaporation duct influence is characterized by its height. In the next generation of propagation models to be introduced into the Fleet, profiles of refractivity in the surface layer will be required for direct calculation of propagation effects. These profiles will be calculated from the same parameters as is the evaporation duct height.

Figure 12 illustrates two modified refractivity profiles taken from the evaporation duct heights calculated from the temperature measurements of the two systems for 0300 GMT, 13 July 1991. This was a time period that represented an extreme in duct height differences between the two sensor systems.

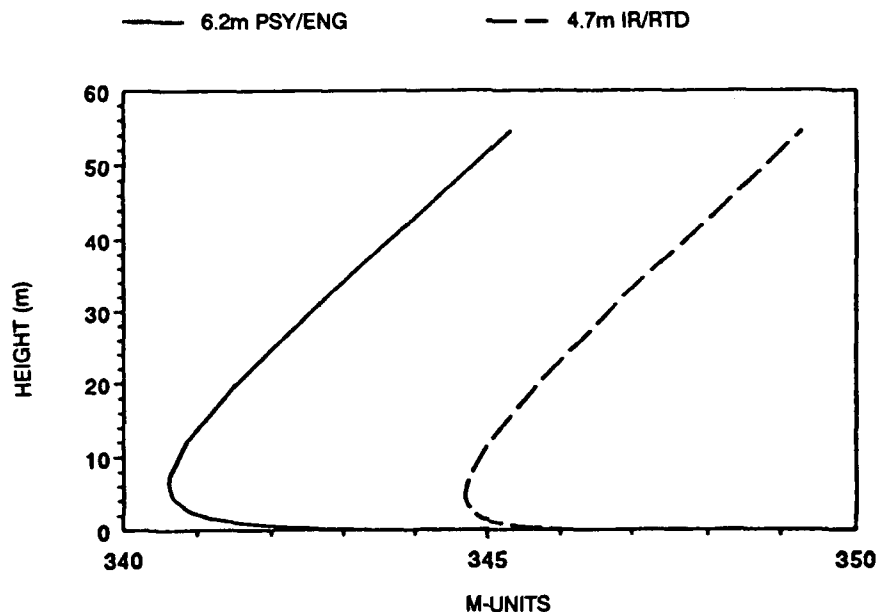


Figure 12. Modified refractive index versus height profiles for 0300 GMT, 13 July 1991. (Psychrometer/engine and IR/RTD sensors.)

These two profiles were provided as input parameters to the Radio Physical-Optic (RPO) propagation program currently being developed at NCCOSC RDT&E Division (Hitney, 1991). Figures 13 through 15 show predicted propagation losses versus ranges for these two environments for an EM system varying in frequency from 3 GHz to 15 GHz. It should be stressed again that the evaporation duct height is a measure of duct strength, not a height below which an antenna must be placed in order to be influenced by the evaporation duct. The frequency-dependent effects of the evaporation duct become more noticeable as the frequency increases between these three figures.

At 15 GHz, the difference in propagation loss between the two environments at a range of 40 kilometers is approximately 10 dB. Assuming an operational scenario of a radar with a performance threshold of 155 dB, this path-loss difference would translate into a detection range of 27.2 kilometers for the 4.7-meter evaporation duct environment versus a 40-kilometer detection range for the 6.2-meter evaporation duct. Assuming these two duct heights were mean heights, it may be argued that for this scenario a detection range difference of 12.0 kilometers is extremely significant.

It has been shown by Dockery (1987), figure 16, that EM signal fluctuations of  $\pm 10$  dB from the mean are common. These fluctuations emphasize the probabilistic nature of detection. In the mean, relative performance is reasonably predictable (Patterson, 1984; Hitney & Vieth, 1990); but a single detection event is not likely to exactly verify the predicted range, even with perfect environmental data. Improvements in

sensors, observational techniques, and data quality control will decrease the variance about the mean. However, the temperatures measured by the IR/RTD produced the lower evaporation duct heights and therefore, would produce the most conservative EM system performance predictions.

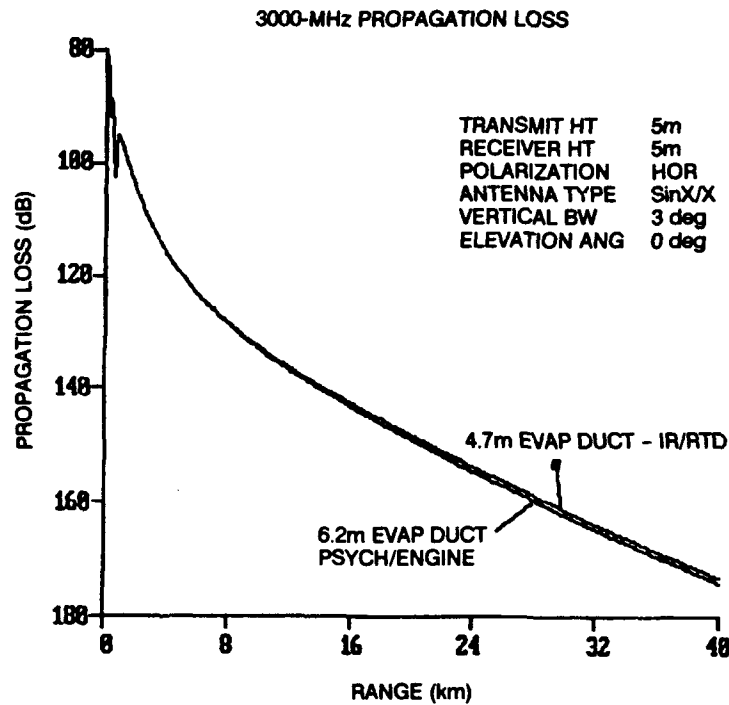


Figure 13. 3-GHz propagation loss within a 4.7- and 6.2-meter evaporation ducting environment.

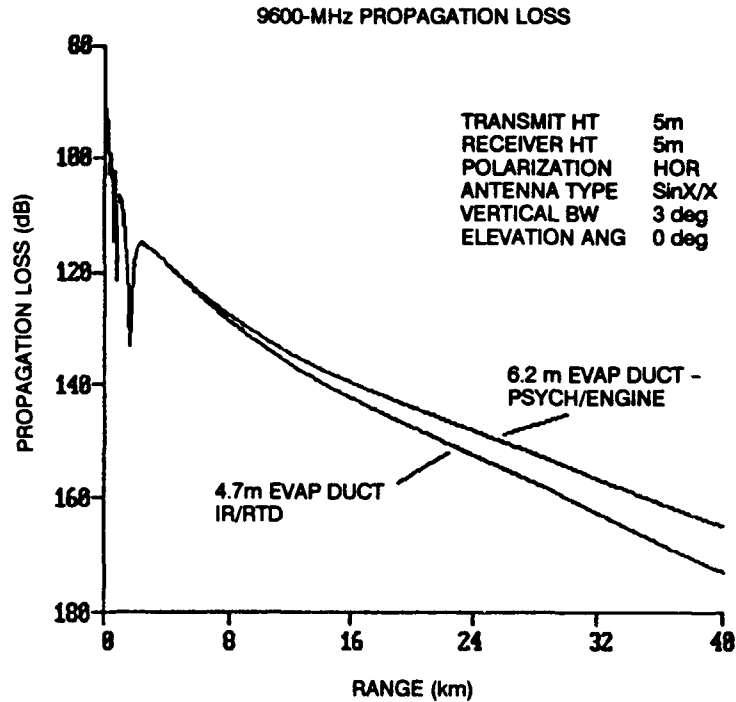


Figure 14. 9.6-GHz propagation loss within a 4.7- and 6.2-meter evaporation ducting environment.

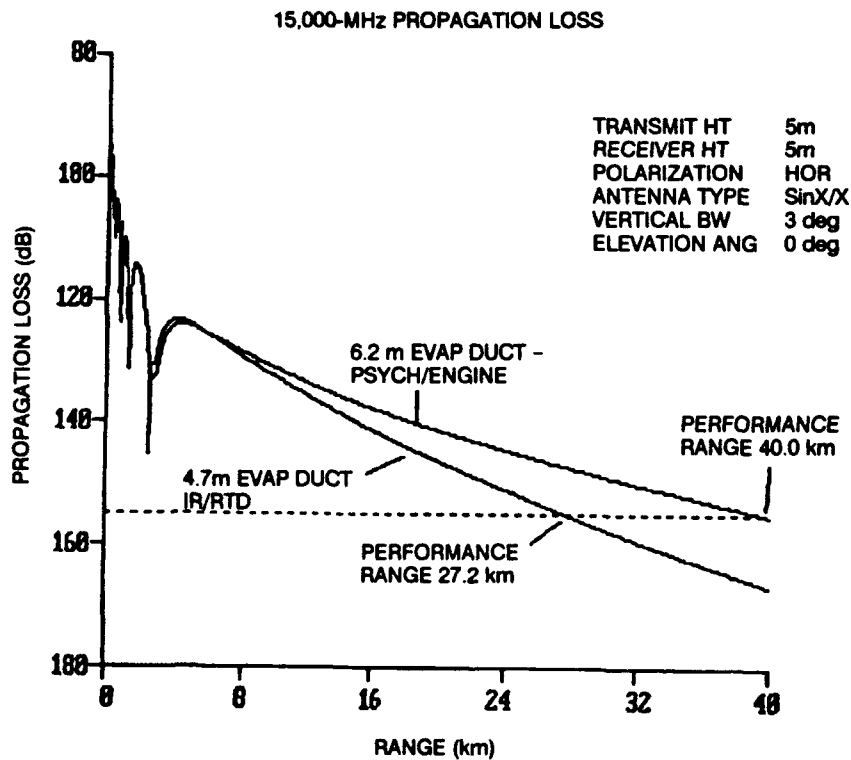


Figure 15. 15-GHz propagation loss within a 4.7- and 6.2-meter evaporation ducting environment.

APL WALLOPS ISLAND EXPERIMENT  
9 OCT 86 1105 - 1121

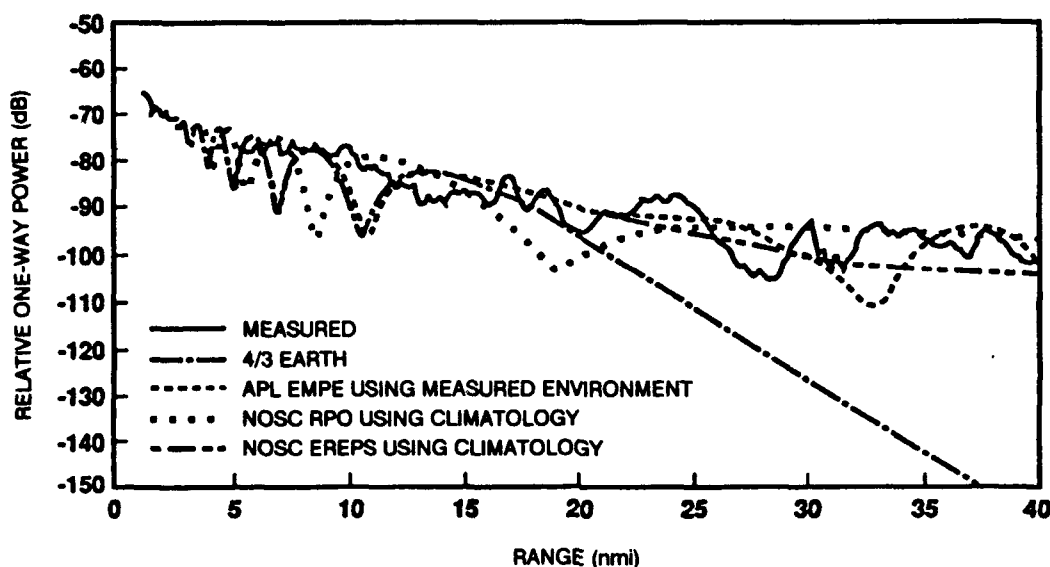


Figure 16. Measured signal strengths about mean signal strength predictions for various propagation models (Dockery, 1987).

## CONCLUSIONS AND RECOMMENDATIONS

a. Environmental measurements indicate the experimental period was under the influence of a single air and water mass. While a small meteorological disturbance passed through the area on 19 July, it was not significant enough to justify a differing air mass. There appears to be no significant difference in the statistical distribution of evaporation duct heights calculated from air and sea-surface temperatures as measured by the psychrometer/engineering intake gauge method and the IR/RTD method.

To separate the influence a single air mass has upon evaporation duct height calculations from the evaporation duct height calculations produced from two different temperature sensing systems, another evaluation should be performed. This second period should ensure that different air and water masses are experienced.

b. While not supported from the evaporation duct height calculations of this experimental period due to the clearly artificial trend in sea-surface temperature reported from the seawater intake, the IR/RTD is the preferred instrument for measuring sea-surface temperature.

c. The nonoperational IR/RTD should be examined to determine the cause of its failure. If found sensitive to RF emissions normally associated with an operational ship, a change in the screening capability of the housing or some sort of grounding technique should be investigated to reduce this sensitivity.

d. The protruding nature of the air-temperature sensor called for increased vigilance in its use. In addition, the mechanism for deploying the sensor failed to operate. The possible relocation of the sensor to a recessed location on the housing or a technique to lubricate the retractable rod should be investigated.

e. An inclusion of a back-lite LCD or an internal light would improve readability during hours of darkness. As an alternative, the air temperature could be stored in the device's memory, as is the IR temperature, to be recalled and displayed once inside a lighted area.

f. The wrist strap and attaching plastic swivel did not withstand normal shipboard use. A modification to the current strap anchor to prevent the inadvertent separation of the strap should be addressed. To free the operator's hands for other tasks and to improve the portability of the IR/RTD, a "shoulder holster" carrying case should be provided.

g. The IR/RTD provides benefits other than data for the calculation of evaporation duct heights. For example, it is useful to determine sea-surface temperatures for use in fog-dissipation forecasts and, in the extreme, it is useful to assess the temperatures of sensitive electronic equipment.

## REFERENCES

- Dockery, G.D. 1987. "Description and Validation of the Electromagnetic Parabolic Equation Propagation Model (EMPE)," Applied Physics Laboratory, Johns Hopkins University FS-87-152, (Sep).
- Hitney, H.V., J. H. Richter, R. A. Pappert, K. D. Anderson, and G. B. Baumgartner, Jr. 1987. "Radio Propagation," *Encyclopedia of Physical Science and Technology*, vol II.
- Hitney, H.V. 1991. "Remote Sensing of Refractivity Structure by Direct Radio Measurements of UHF," Advisory Group for Aerospace Research and Development, 49th Symposium of the Electromagnetic Wave Propagation Panel, (Sep).
- Hitney, H.V., and R. Vieth. 1990. "Statistical Assessment of Evaporation Duct Propagation," *IEEE Transactions on Antennas and Propagation*, vol. 38, no. 6, (Jun).
- Olson, J. 1989. "Shipboard Measurements of Air-Sea Temperature in the Evaporation Duct," NOSC TR 1313 (Dec). Naval Ocean Systems Center, San Diego, CA.
- Patterson, W.L. 1984. "A Comparison of Evaporation Duct Models for IREPS," NOSC TR 960 (Jun). Naval Ocean Systems Center, San Diego, CA.
- Patterson, W.L. 1987. "Historical Electromagnetic Propagation Condition Database Description," NOSC TD 1149 (Sep). Naval Ocean Systems Center, San Diego, CA.
- Paulus, R.A. 1984. "Practical Application of the IREPS Evaporation Duct Model," NOSC TR 966 (Jun). Naval Ocean Systems Center, San Diego, CA.

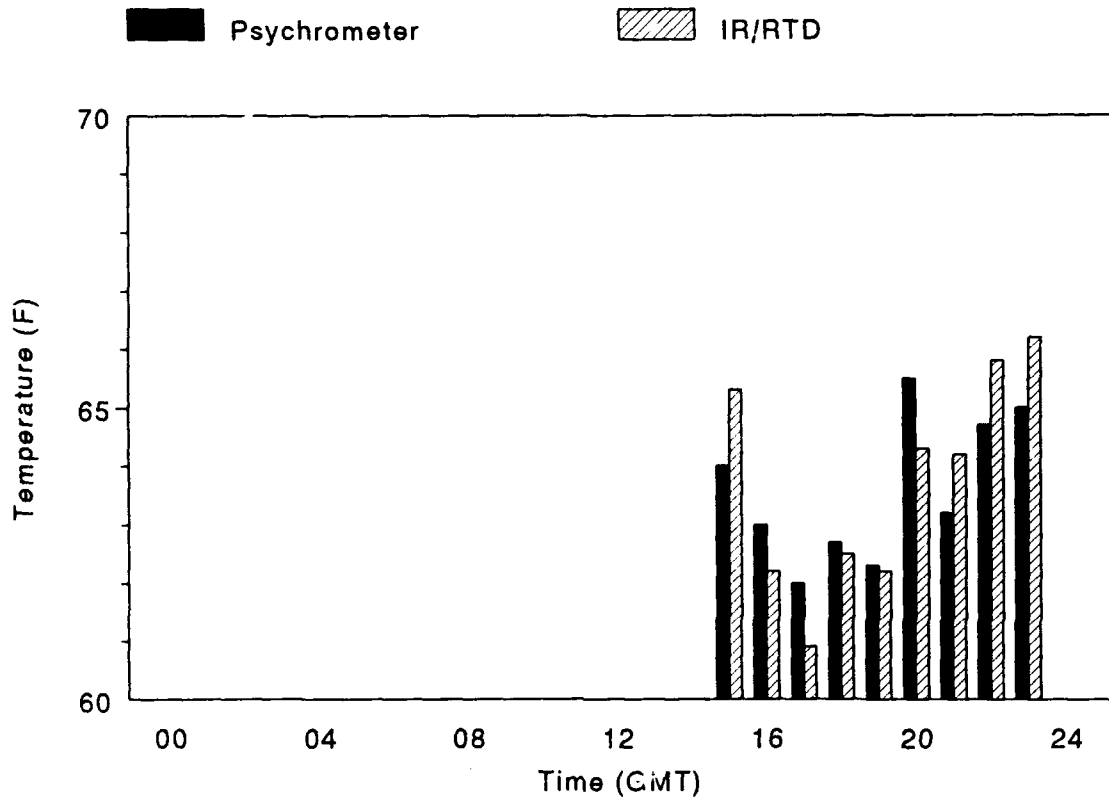
**APPENDIX A**

**AIR AND SEA-SURFACE TEMPERATURES, AIR/SEA-SURFACE  
TEMPERATURE DIFFERENCES, AND COMPUTED EVAPORATION  
DUCT HEIGHTS, 12-24 JULY 1991**



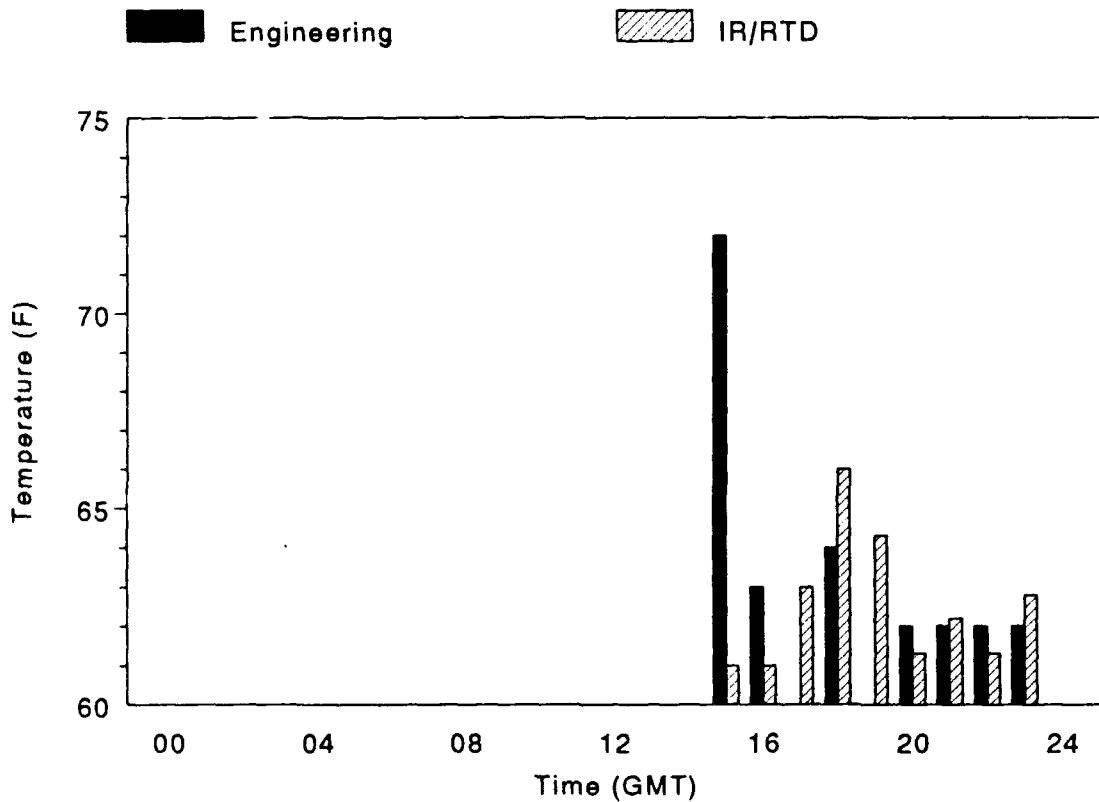
## Air Temperature

July 12, 1991



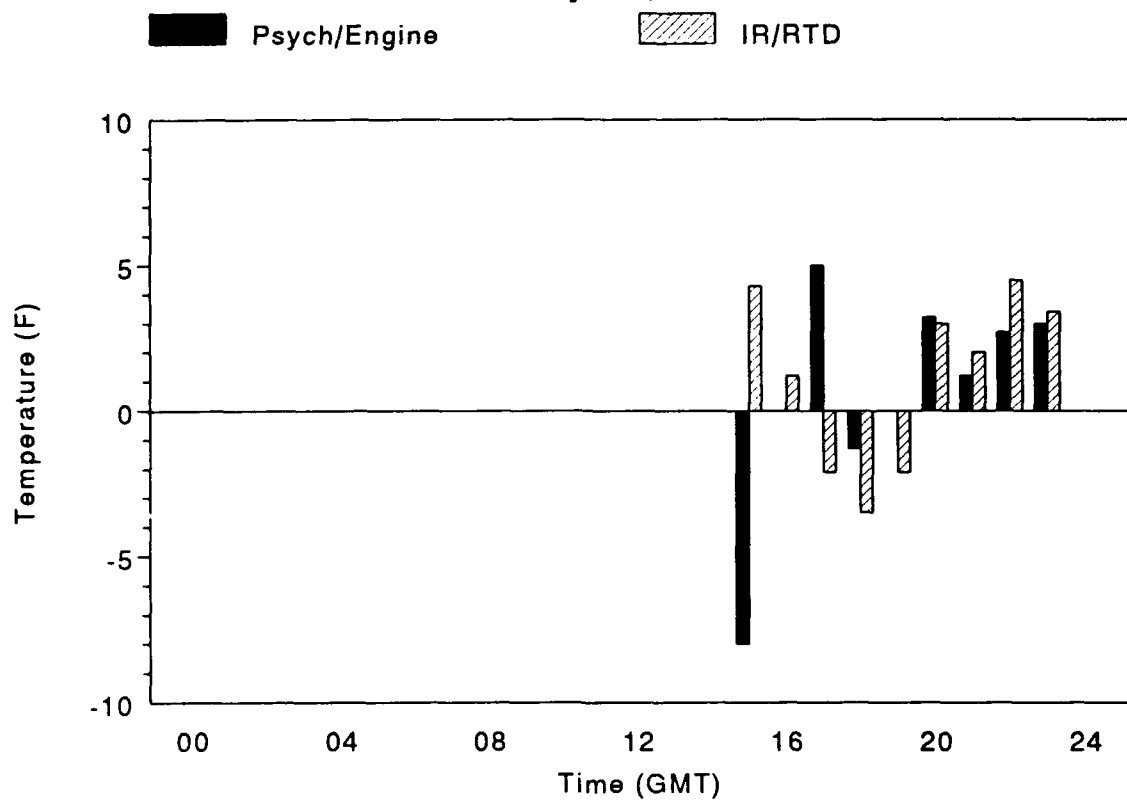
## Sea-surface Temperature

July 12, 1991



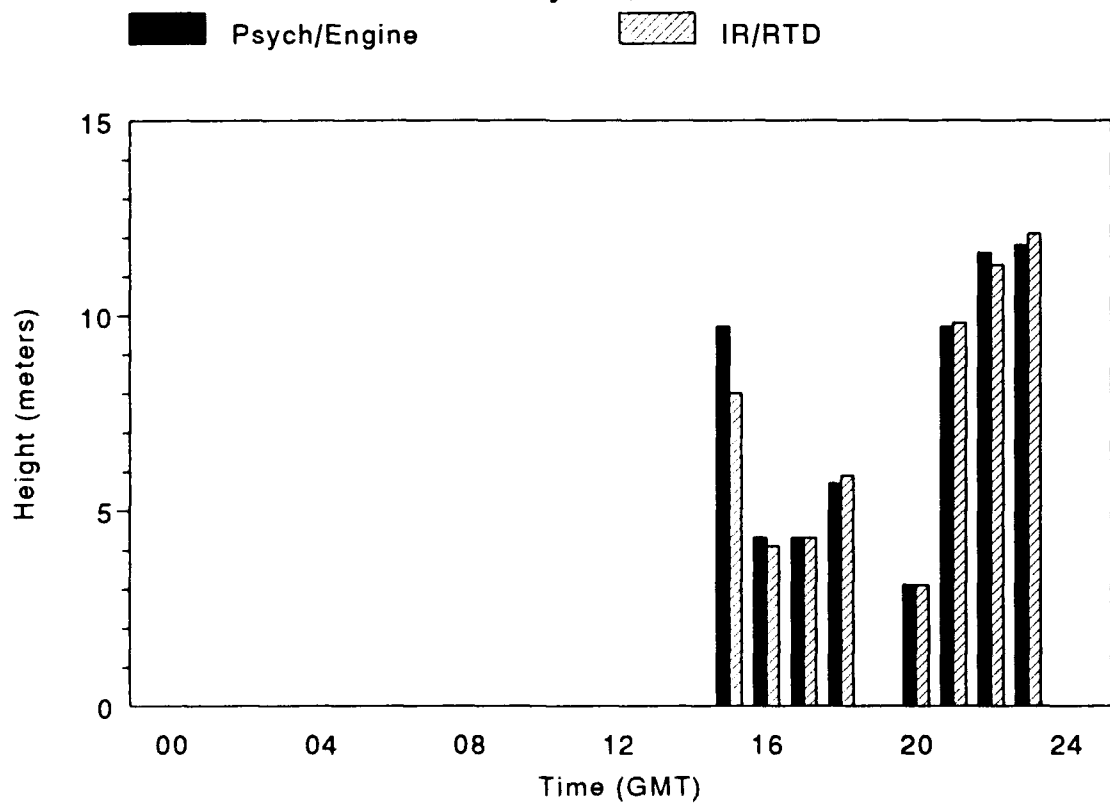
# Air/Sea-surface Temperature Difference

July 12, 1991



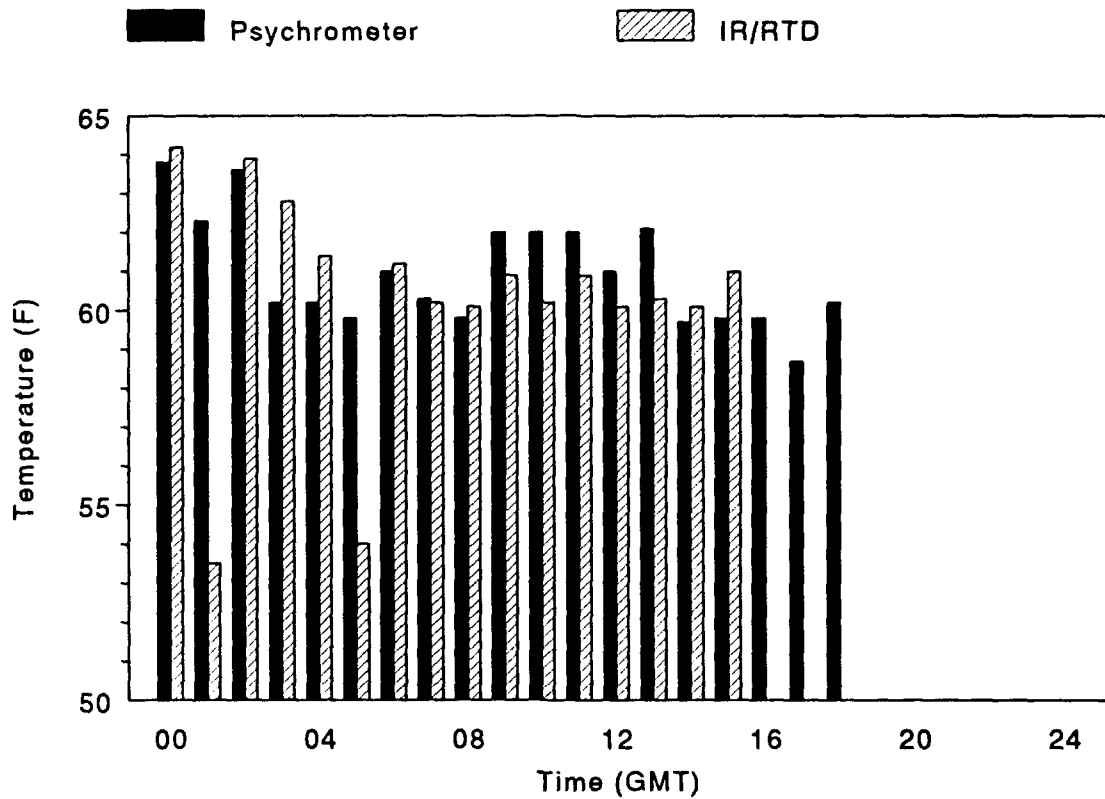
# Evaporation Duct Height

July 12, 1991



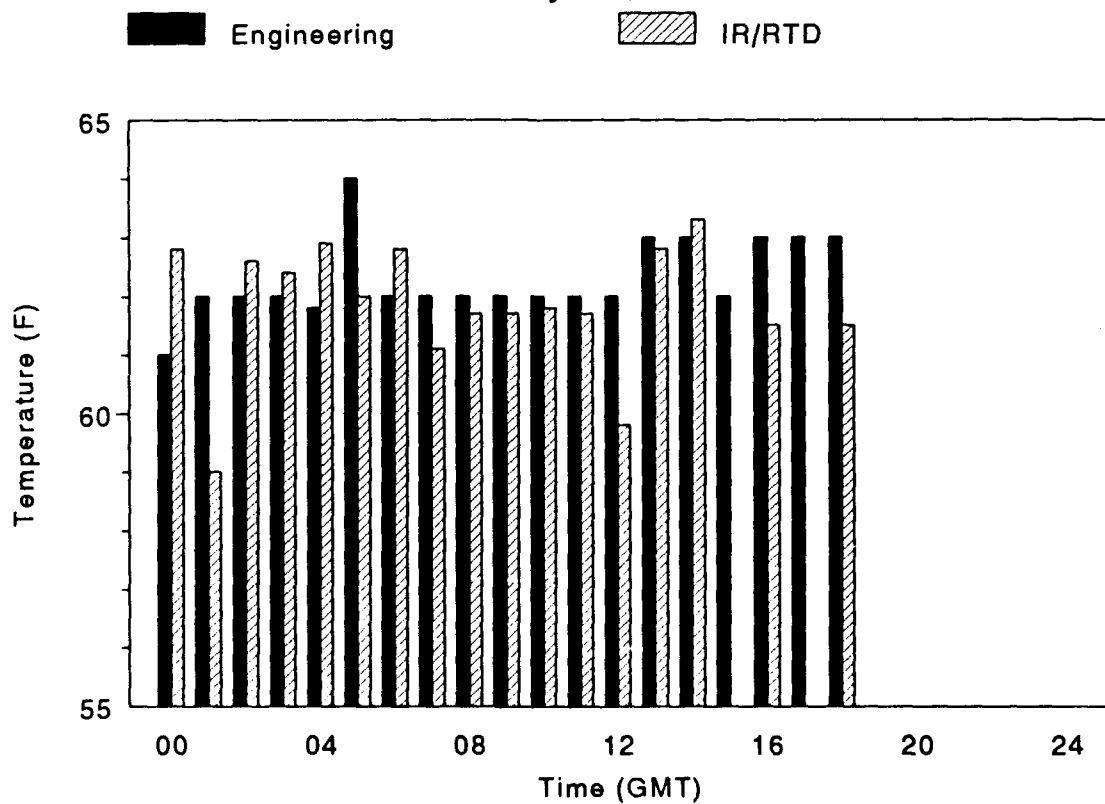
## Air Temperature

July 13, 1991



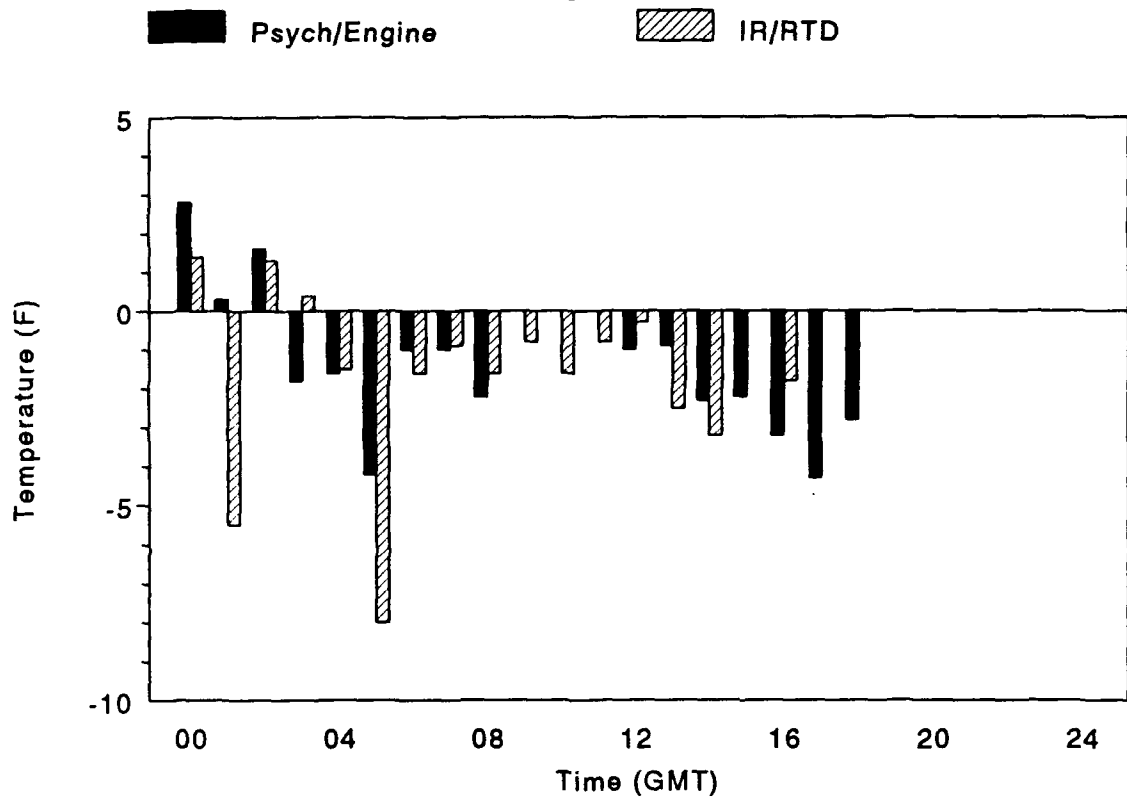
## Sea-surface Temperature

July 13, 1991



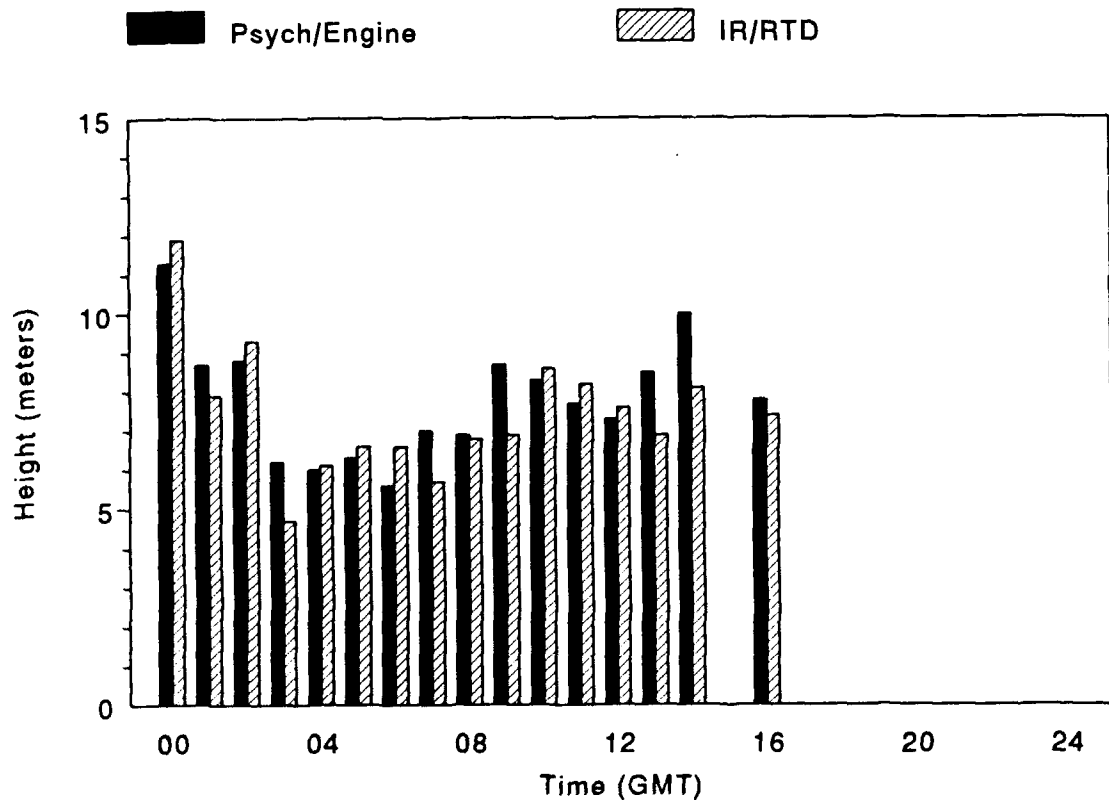
# Air/Sea-surface Temperature Difference

July 13, 1991



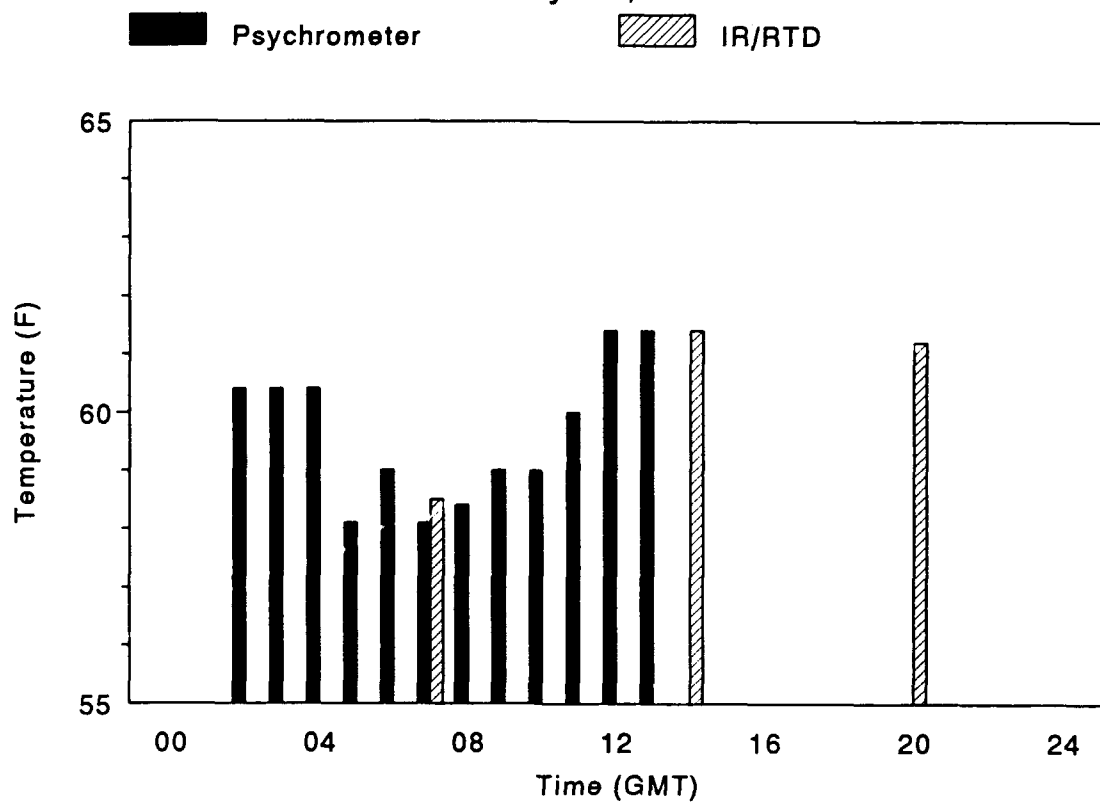
# Evaporation Duct Height

July 13, 1991



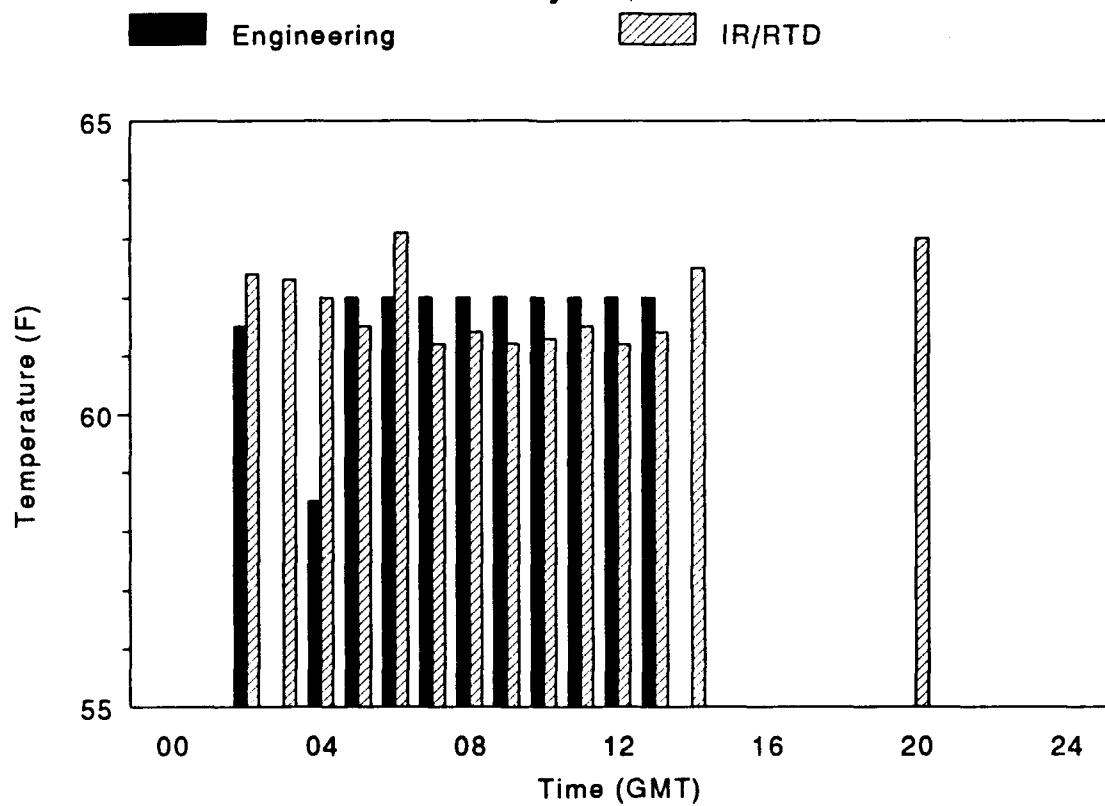
## Air Temperature

July 14, 1991



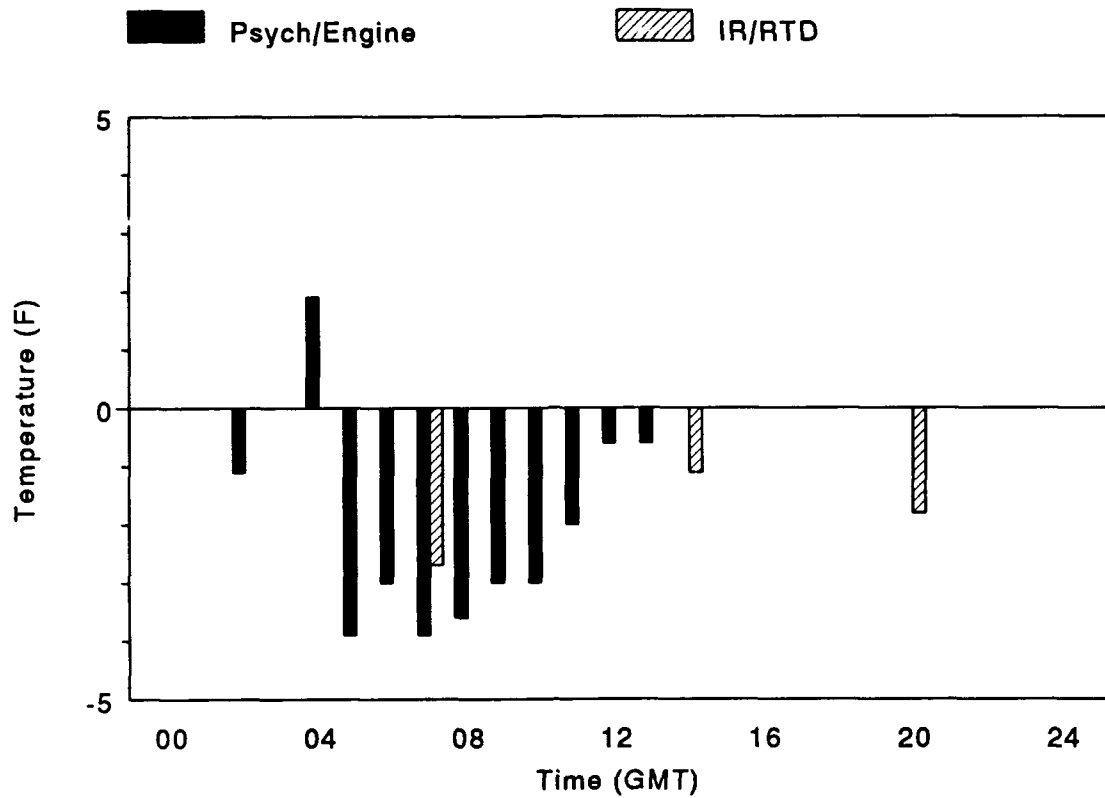
## Sea-surface Temperature

July 14, 1991



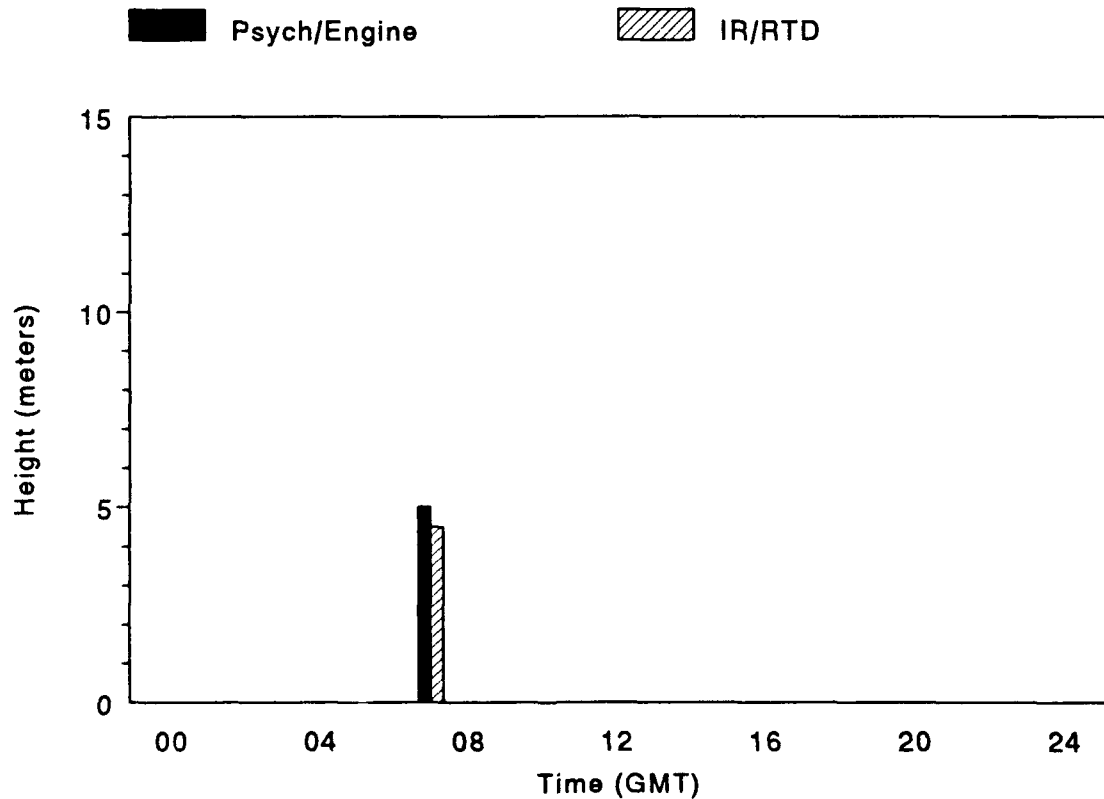
## Air/Sea-surface Temperature Difference

July 14, 1991



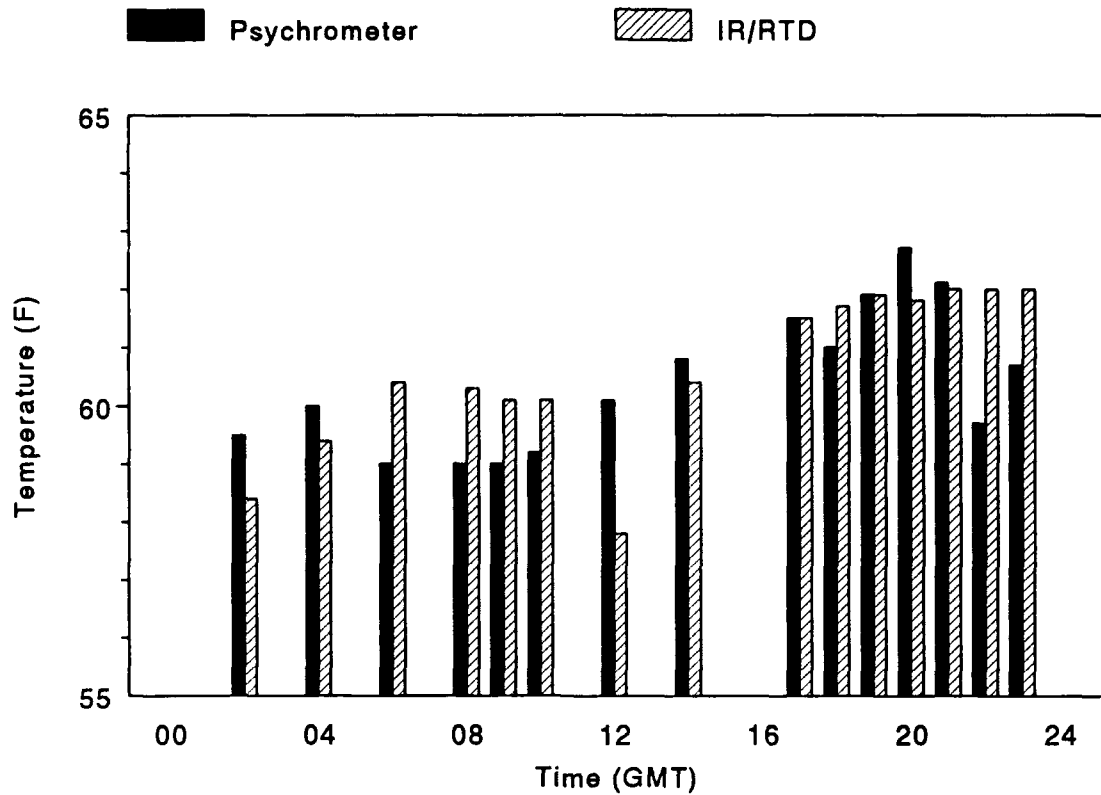
## Evaporation Duct Height

July 14, 1991



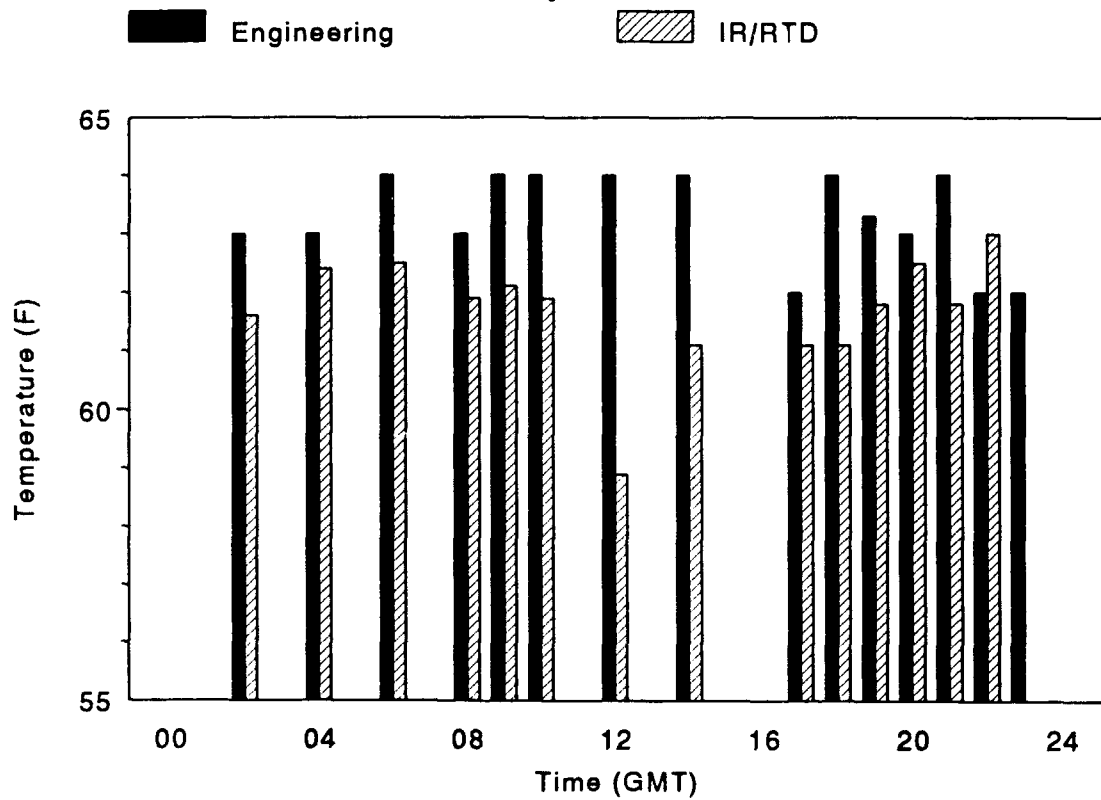
## Air Temperature

July 15, 1991



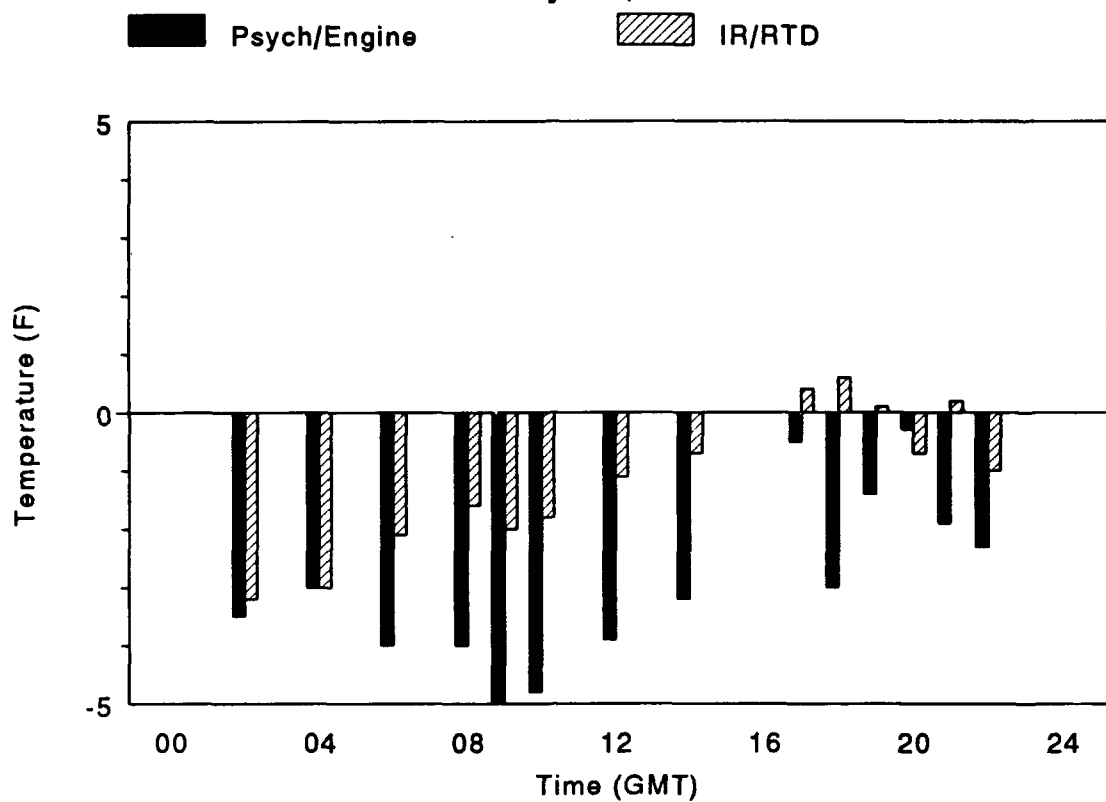
## Sea-surface Temperature

July 15, 1991



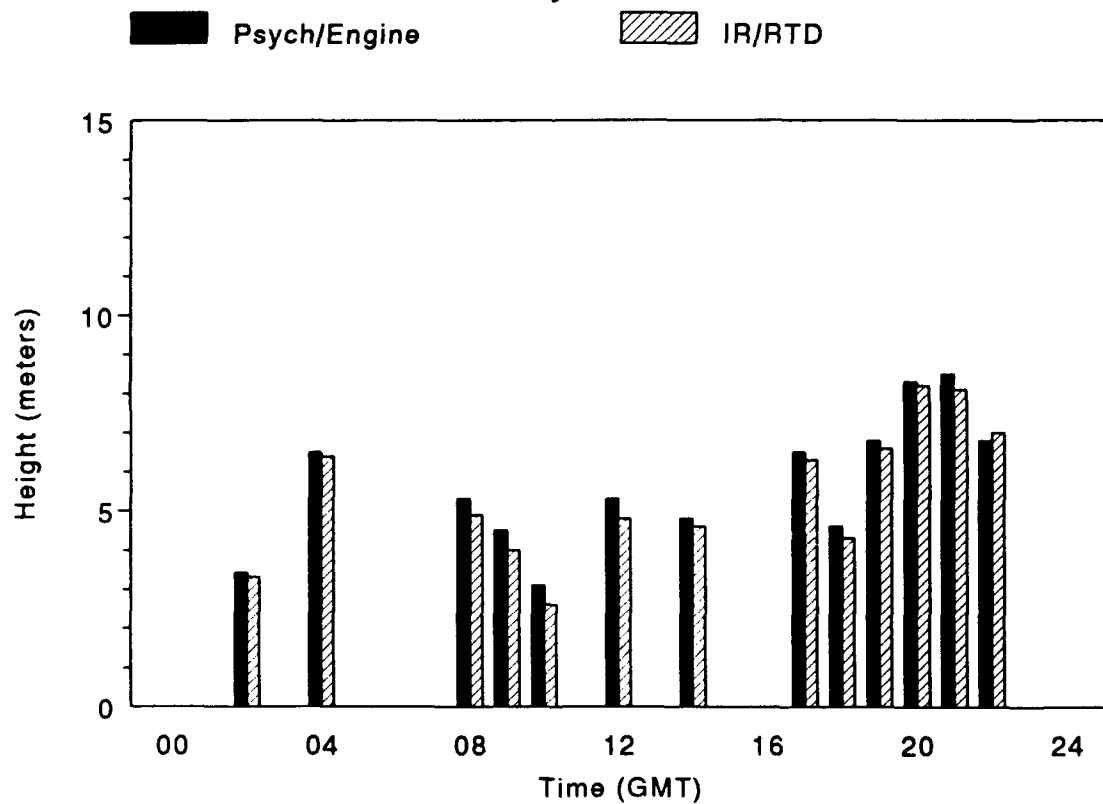
# Air/Sea-surface Temperature Difference

July 15, 1991



# Evaporation Duct Height

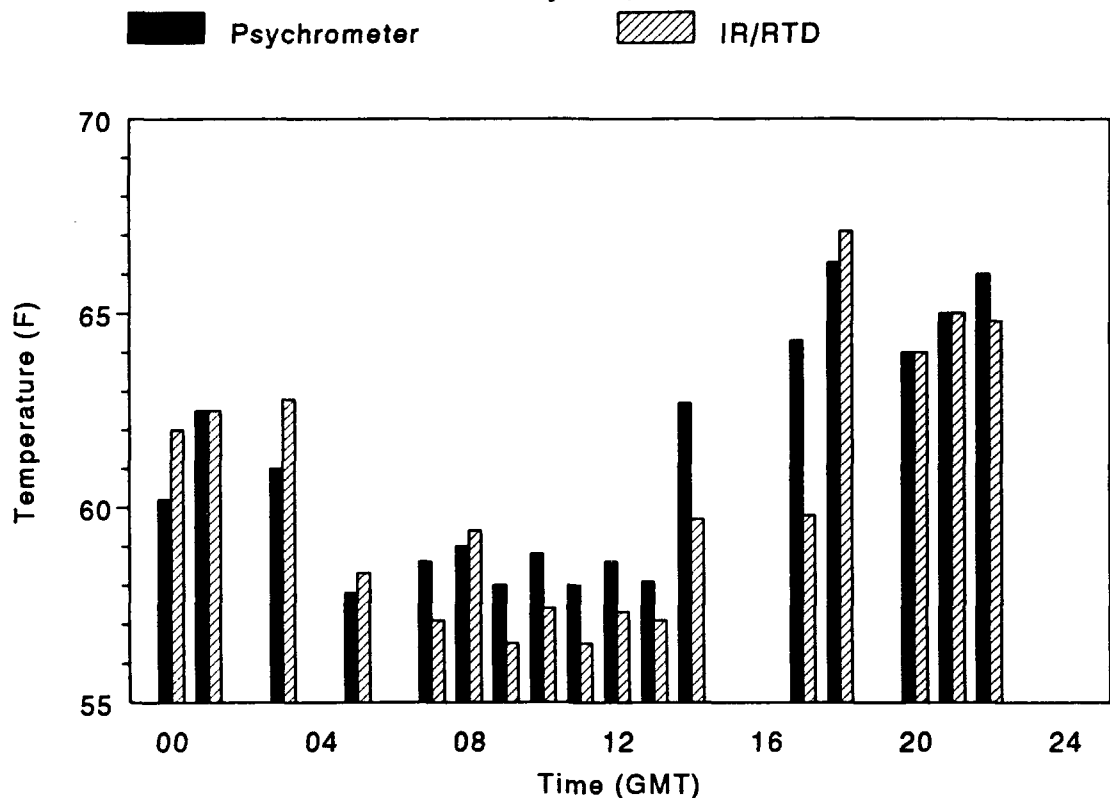
July 15, 1991





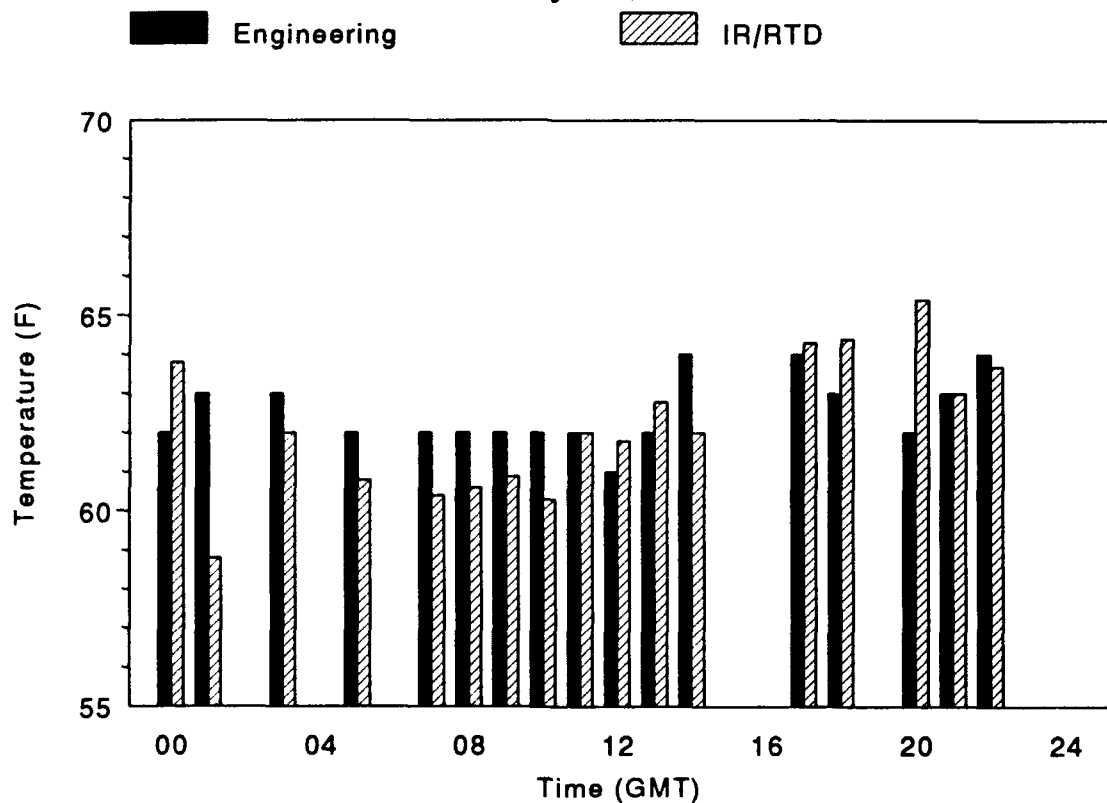
# Air Temperature

July 16, 1991



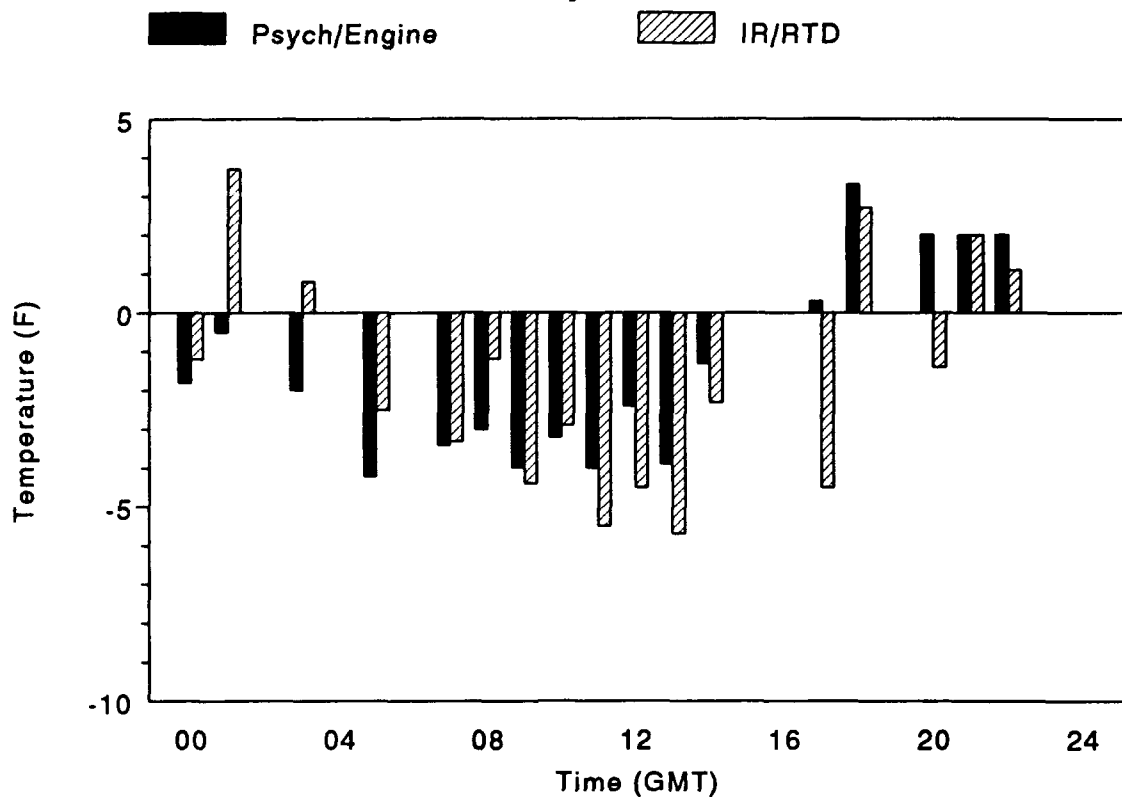
# Sea-surface Temperature

July 16, 1991



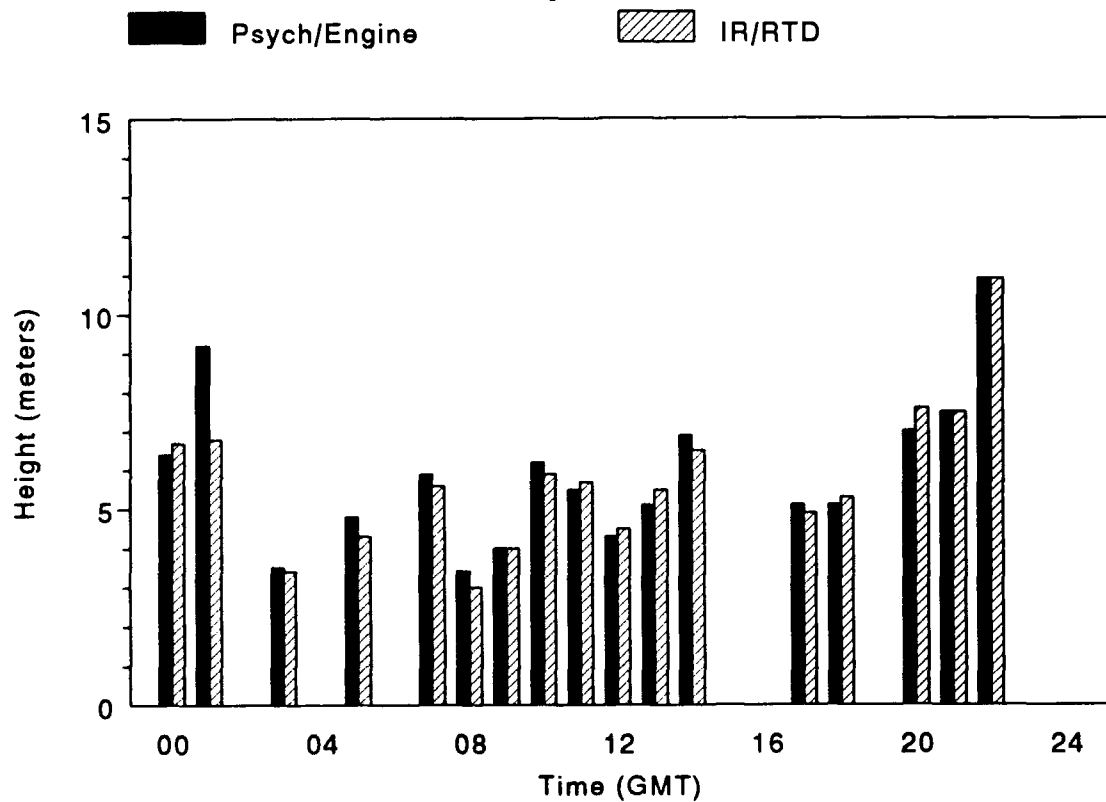
# Air/Sea-surface Temperature Difference

July 16, 1991



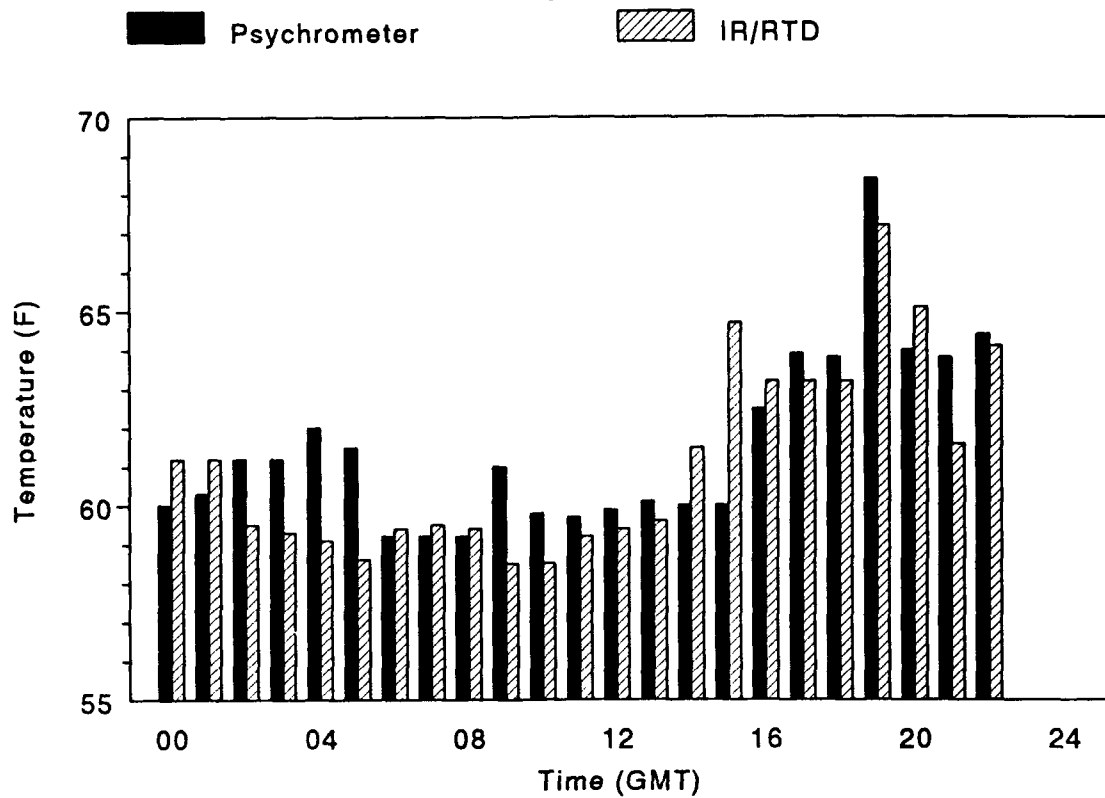
# Evaporation Duct Height

July 16, 1991



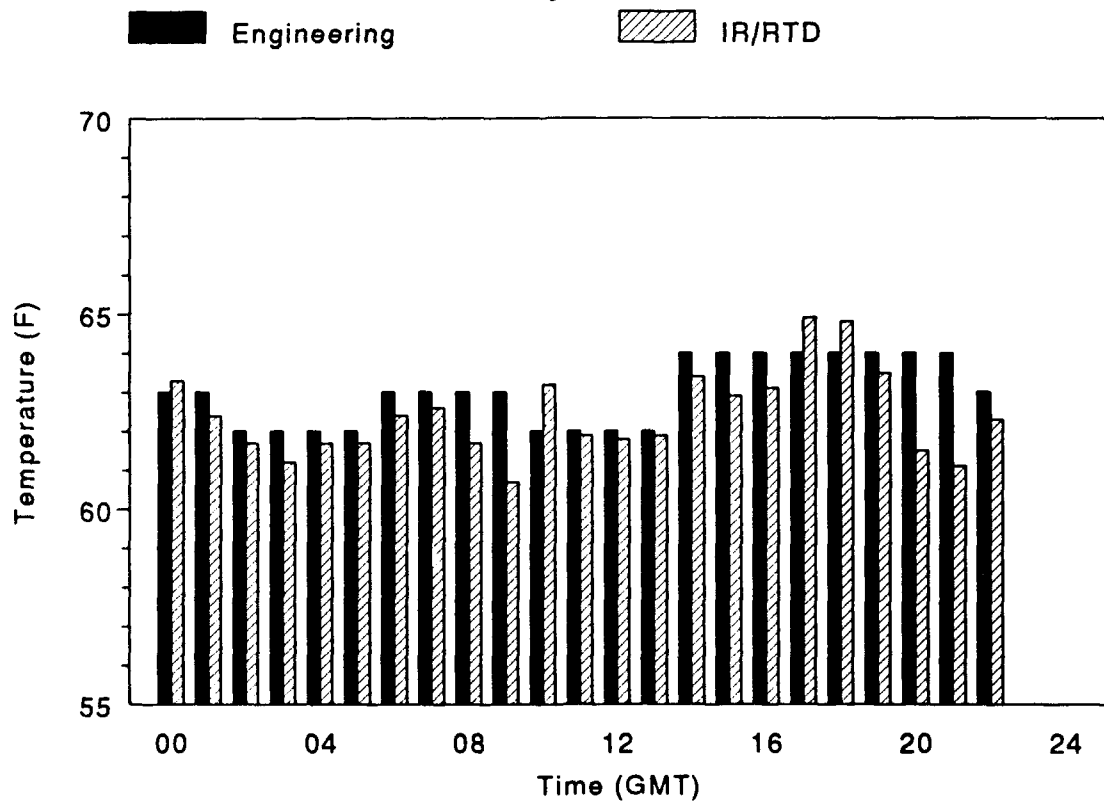
## Air Temperature

July 17, 1991



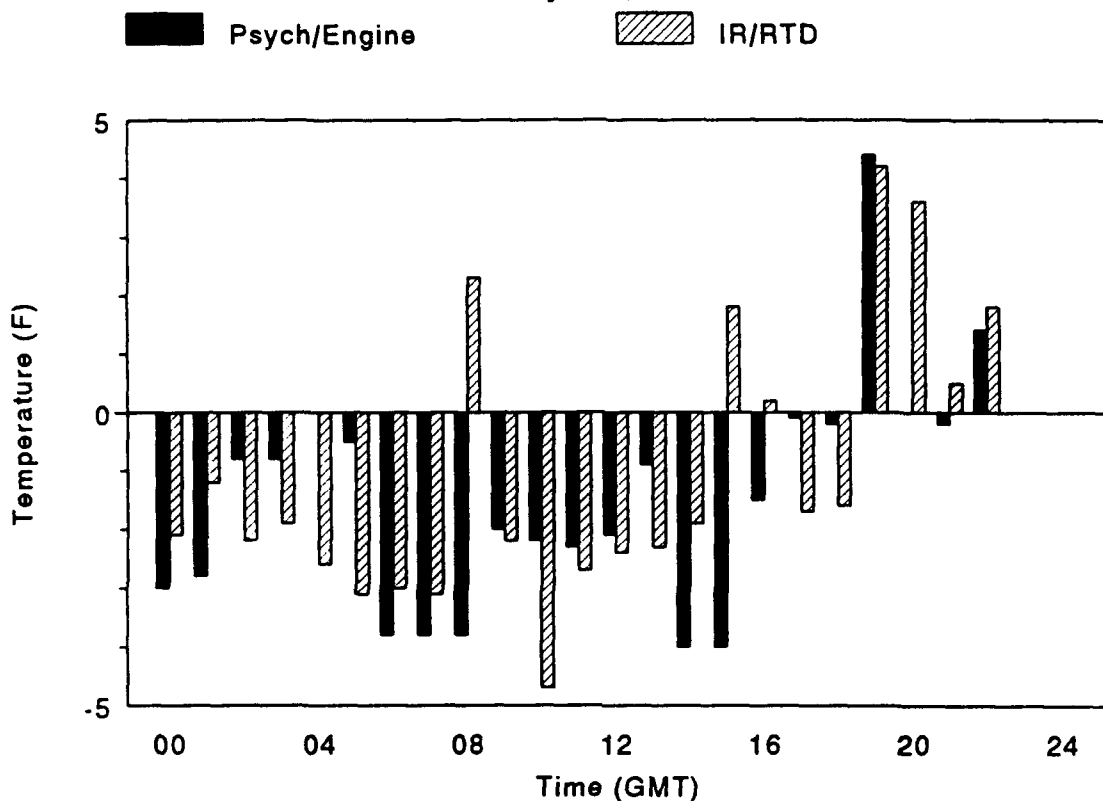
## Sea-surface Temperature

July 17, 1991



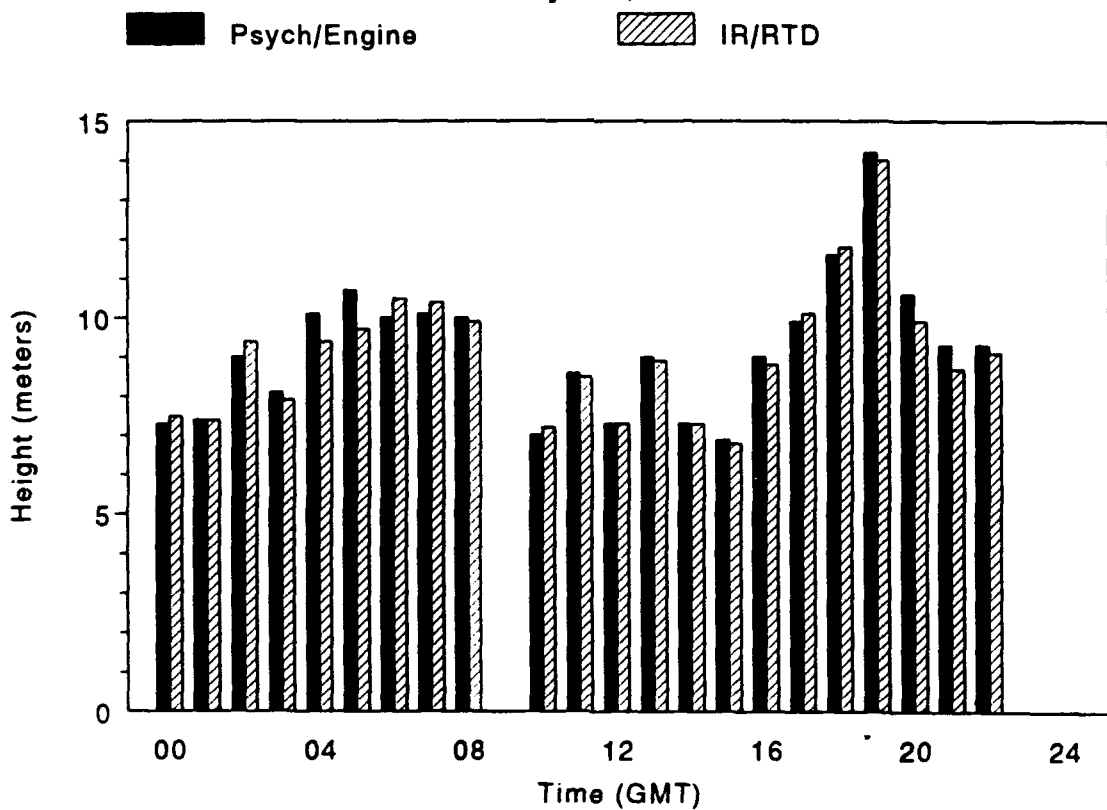
# Air/Sea-surface Temperature Difference

July 17, 1991



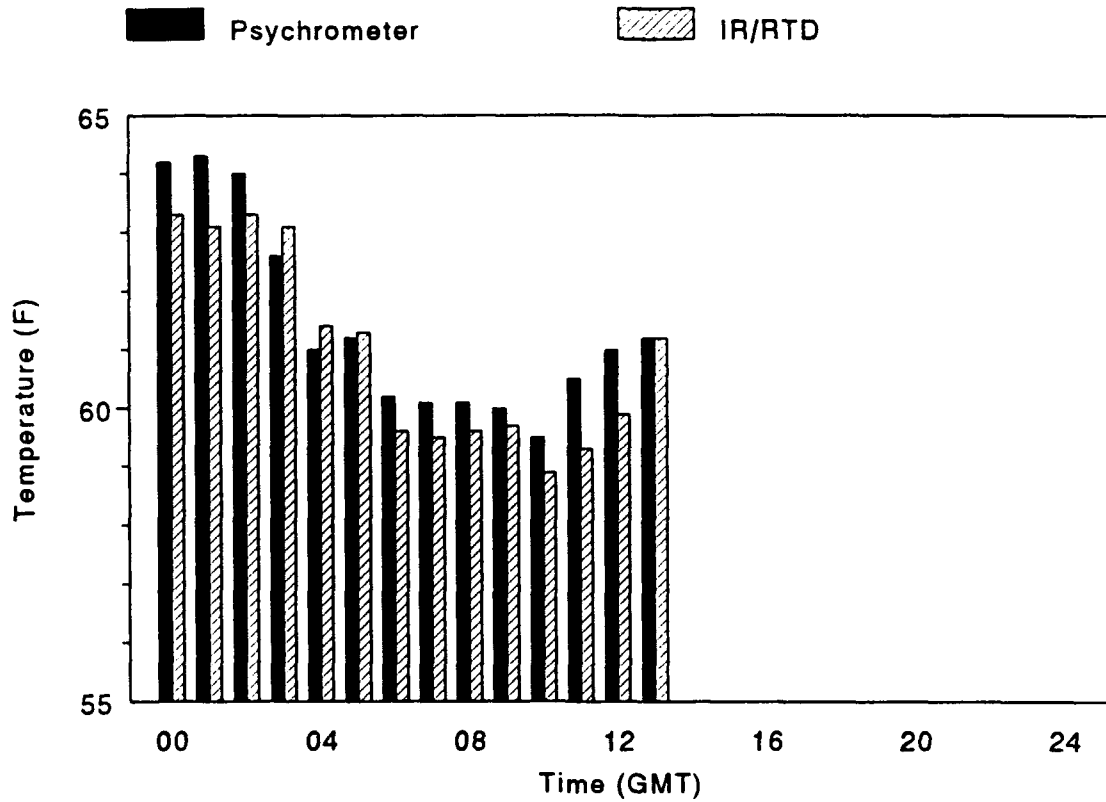
# Evaporation Duct Height

July 17, 1991



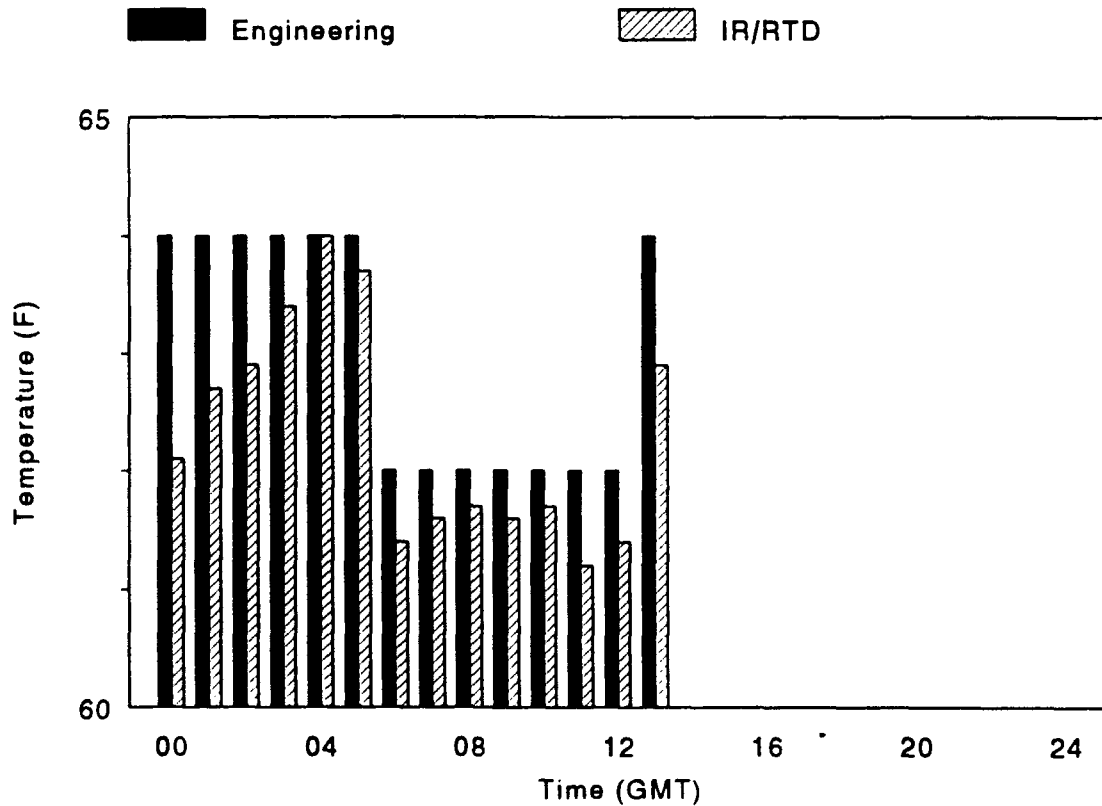
## Air Temperature

July 18, 1991



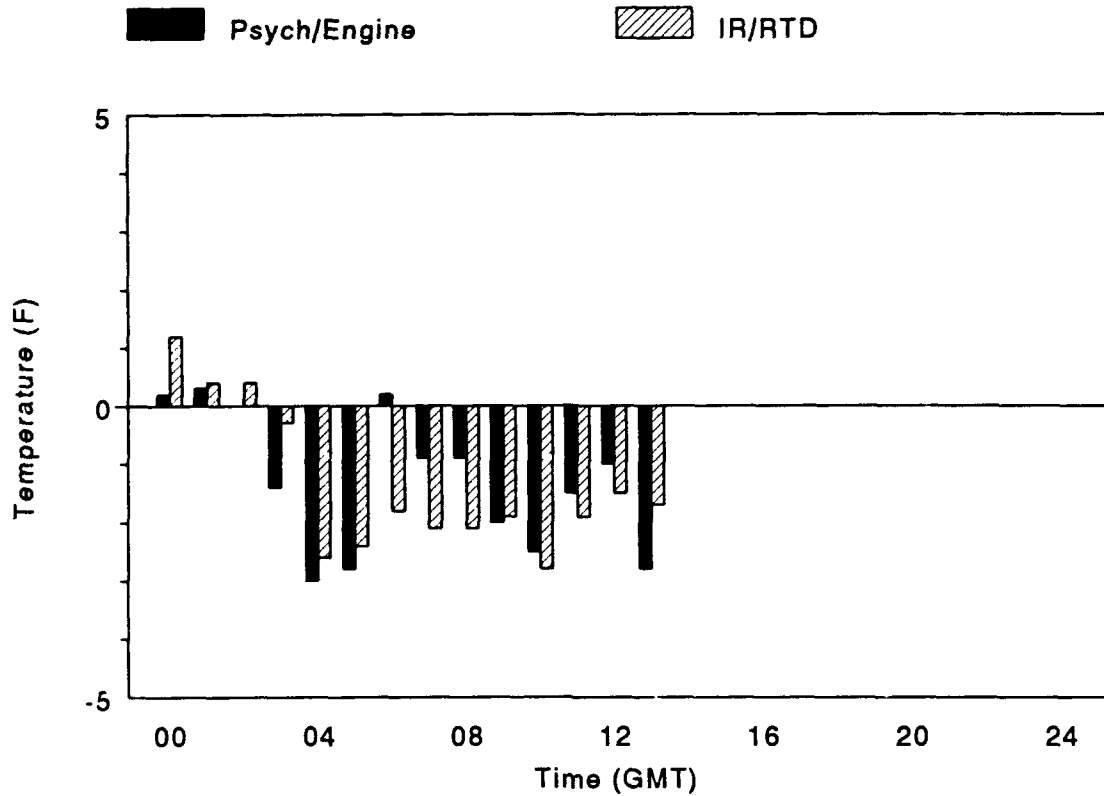
## Sea-surface Temperature

July 18, 1991



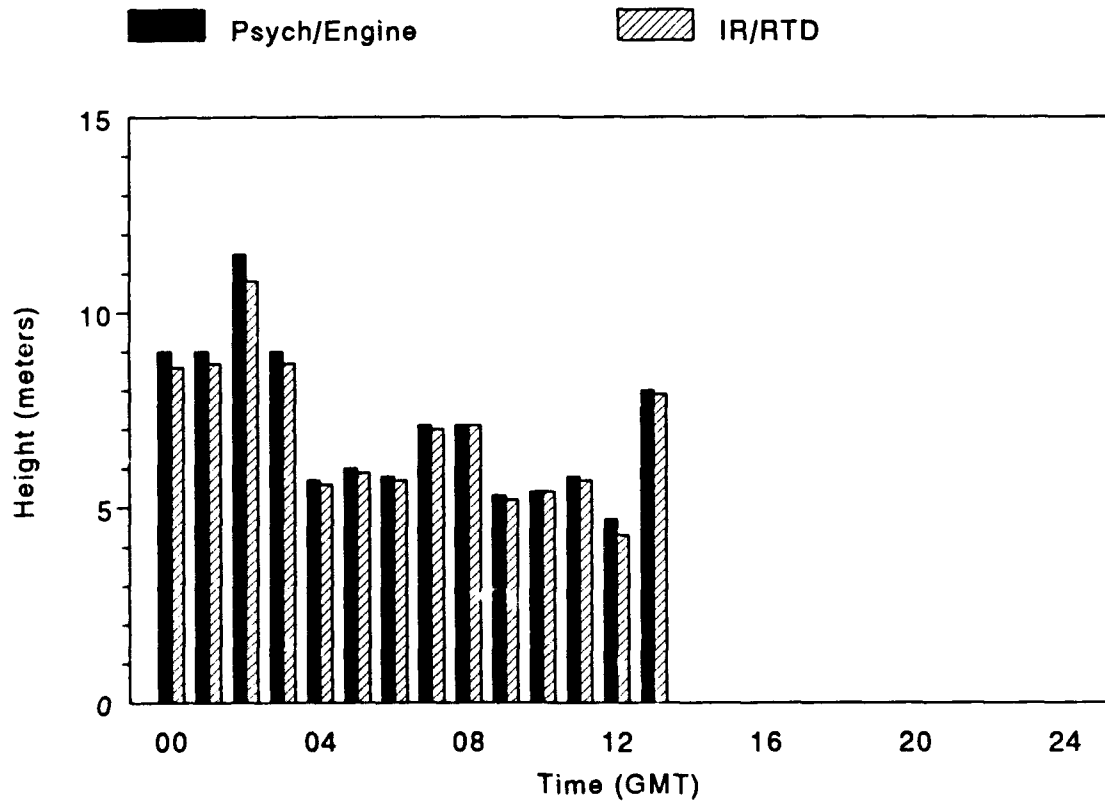
# Air/Sea-surface Temperature Difference

July 18, 1991



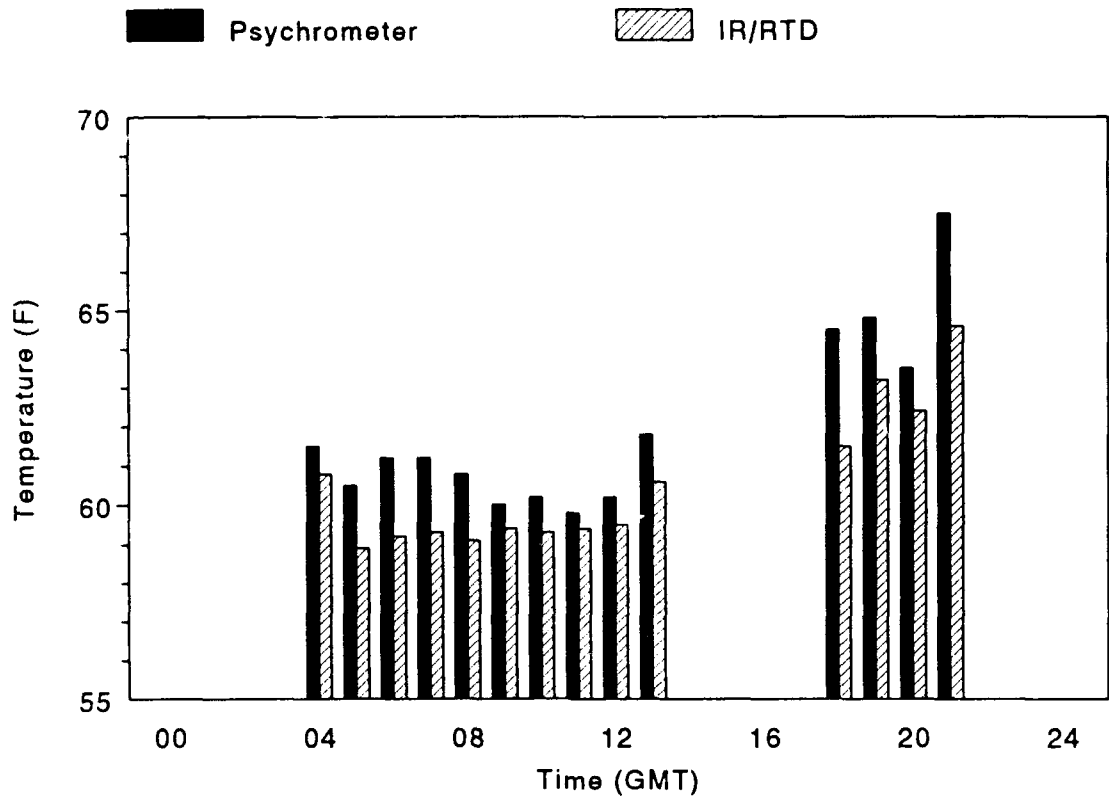
# Evaporation Duct Height

July 18, 1991



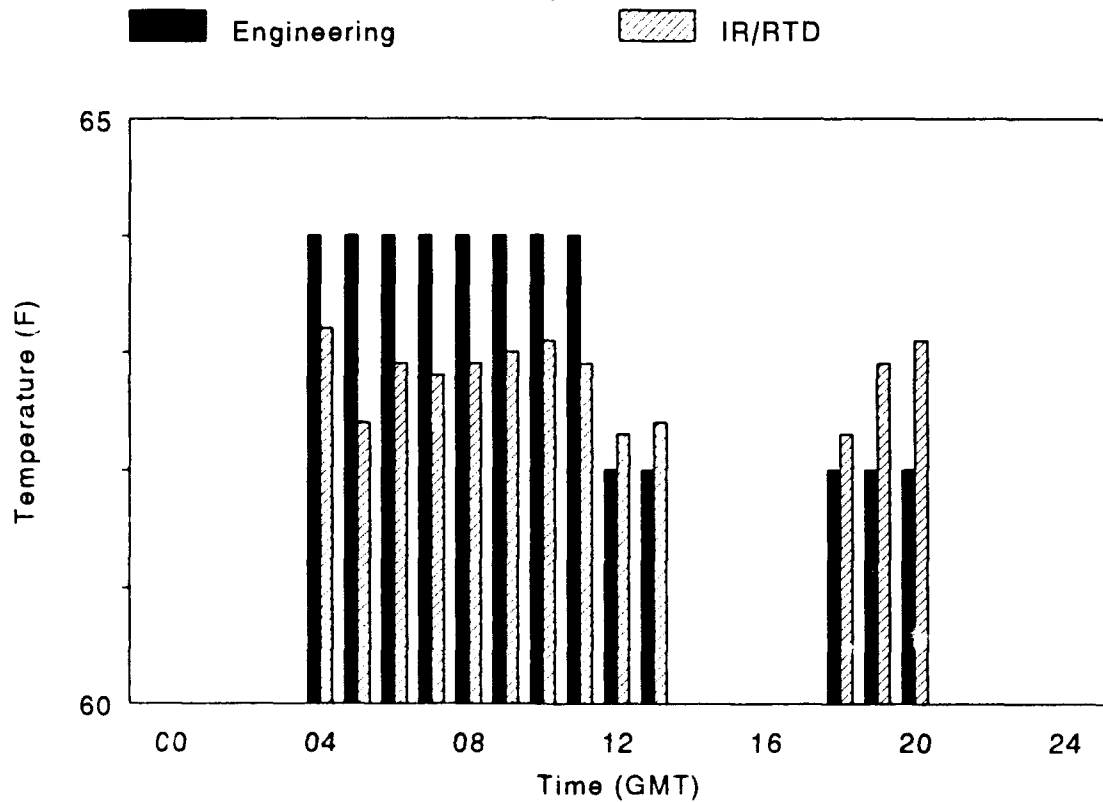
# Air Temperature

July 19, 1991



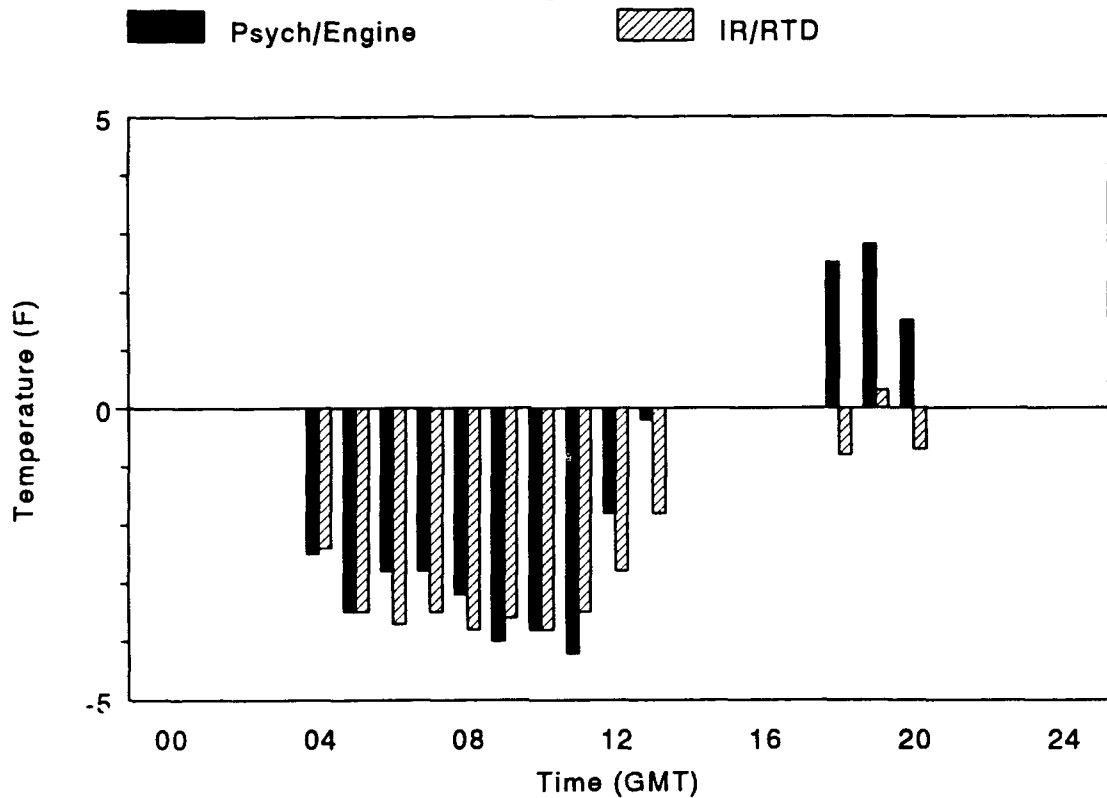
# Sea-surface Temperature

July 19, 1991



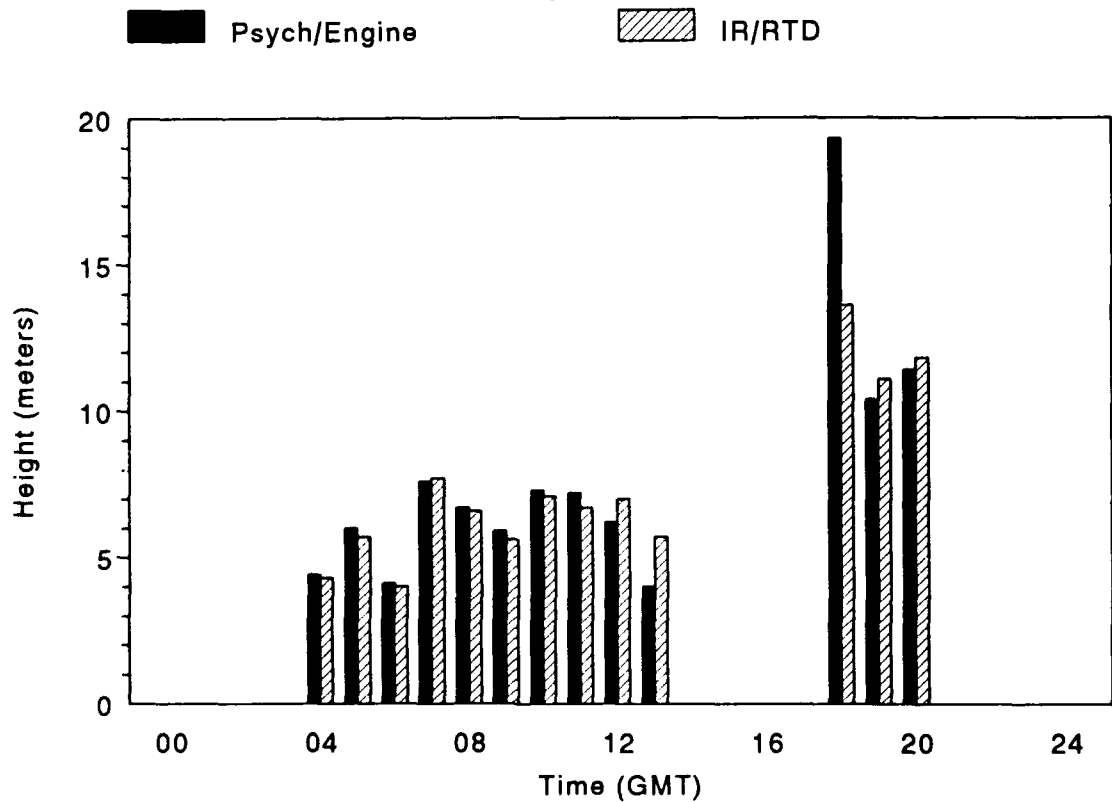
# Air/Sea-surface Temperature Difference

July 19, 1991



# Evaporation Duct Height

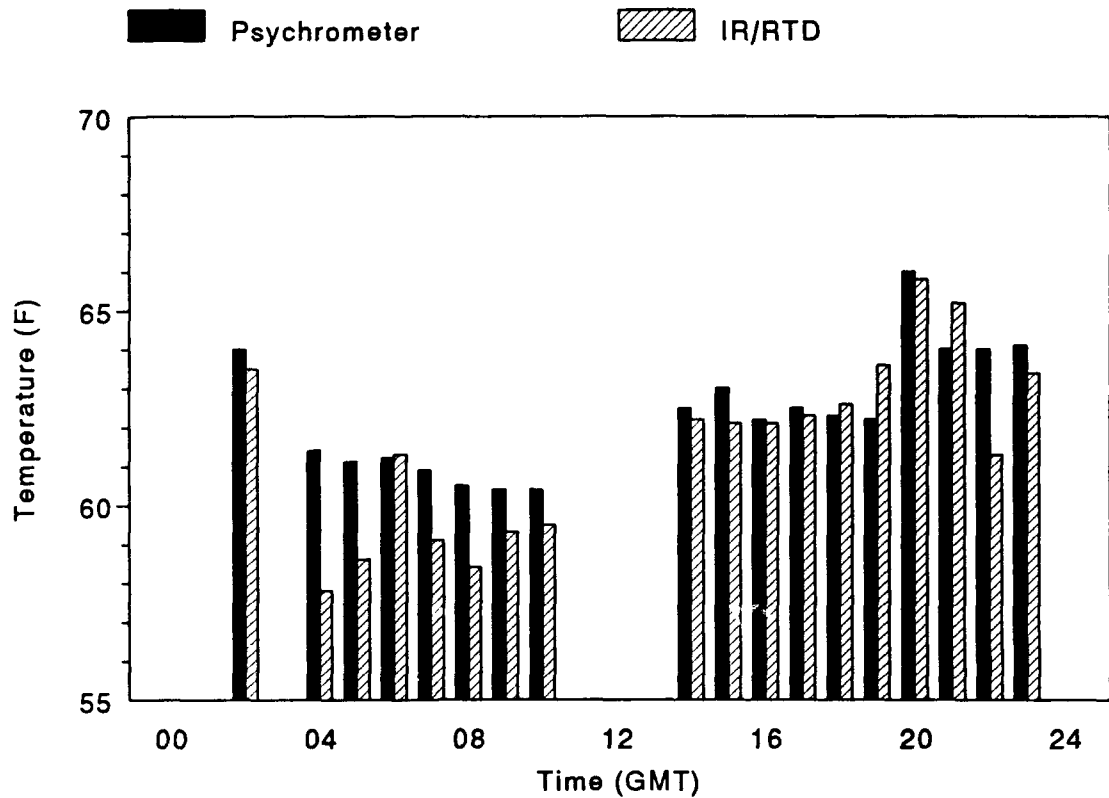
July 19, 1991





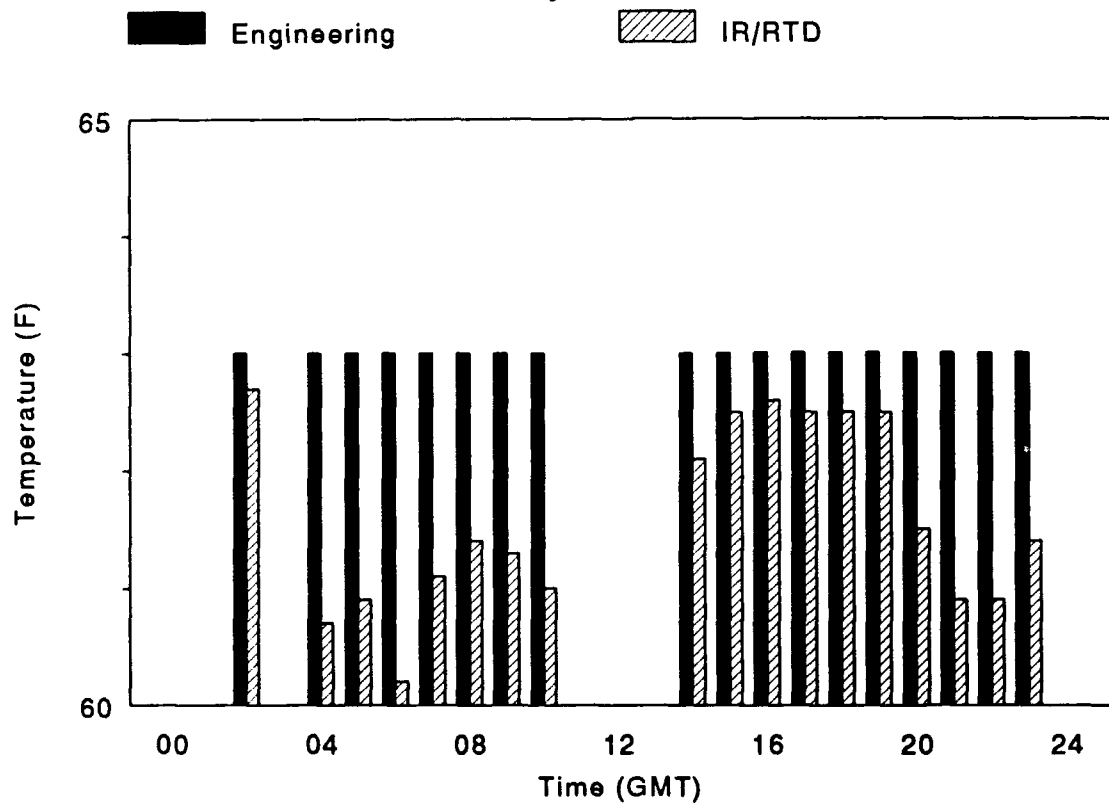
## Air Temperature

July 20, 1991



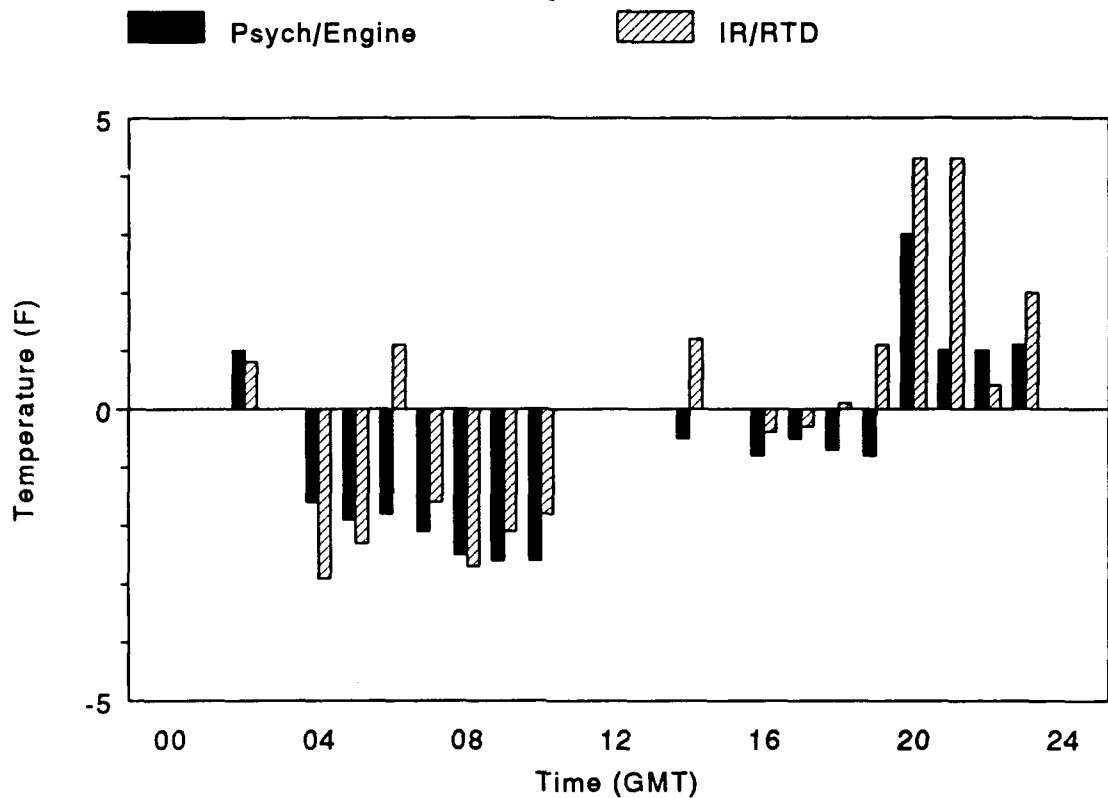
## Sea-surface Temperature

July 20, 1991



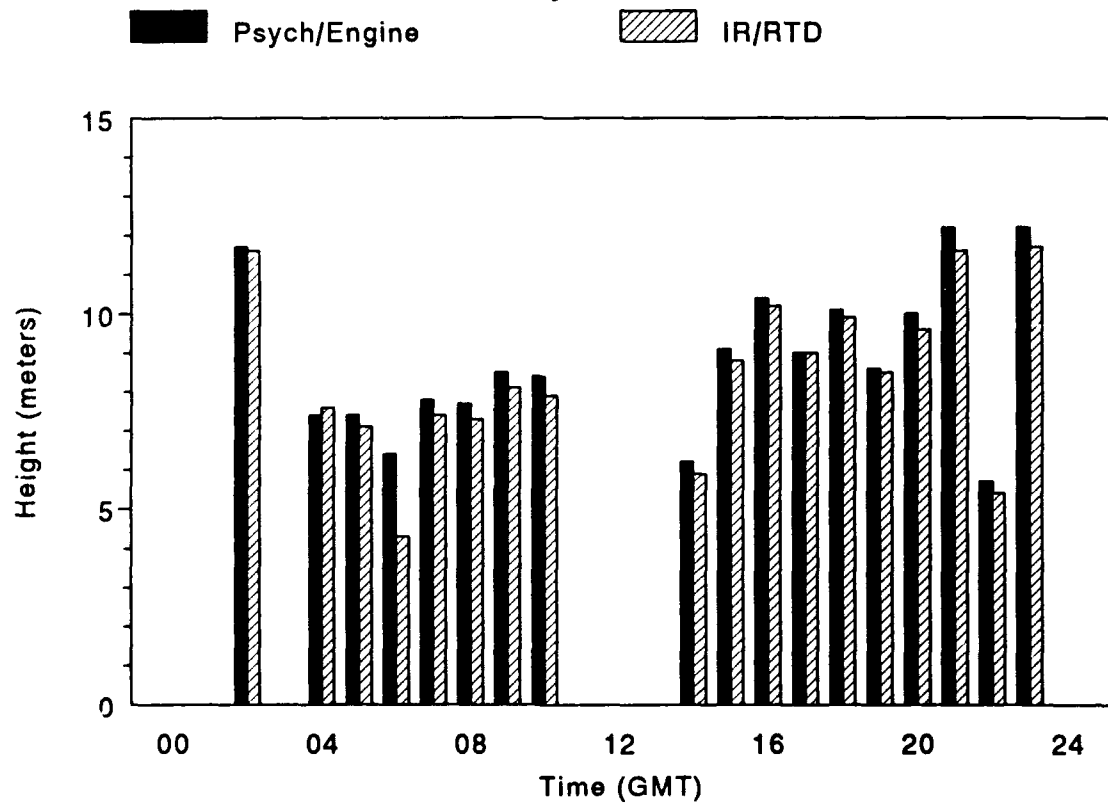
# Air/Sea-surface Temperature Difference

July 20, 1991



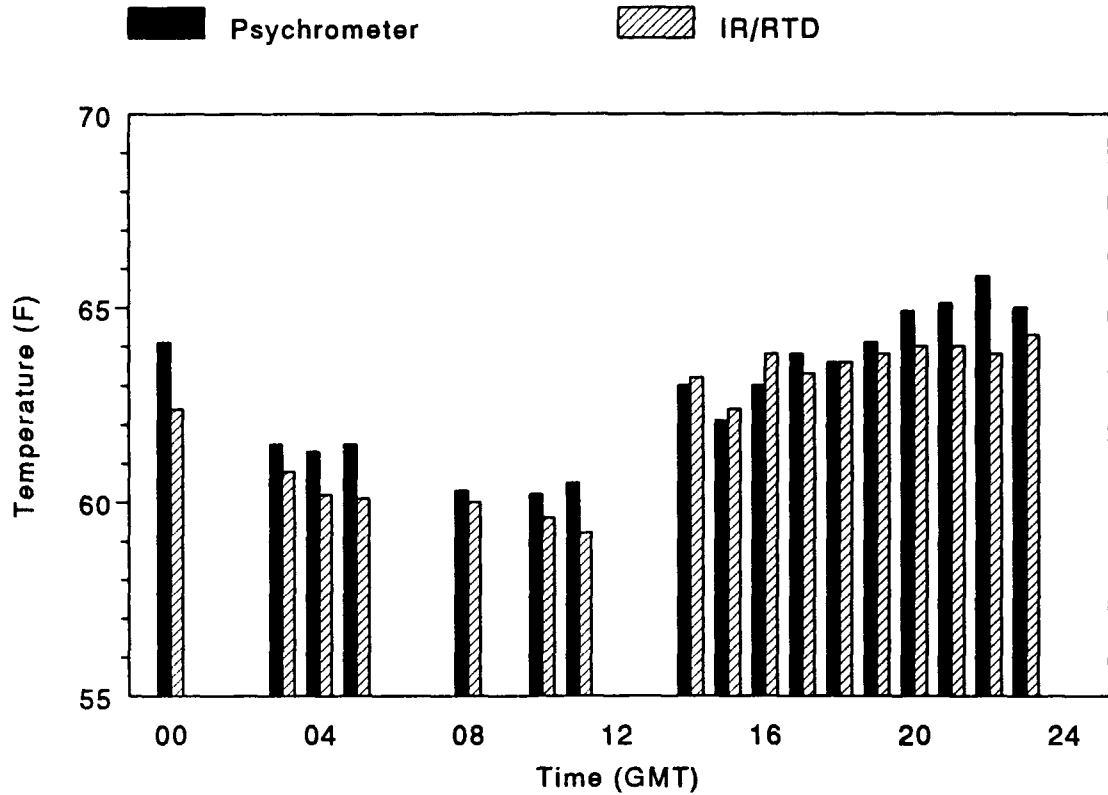
# Evaporation Duct Height

July 20, 1991



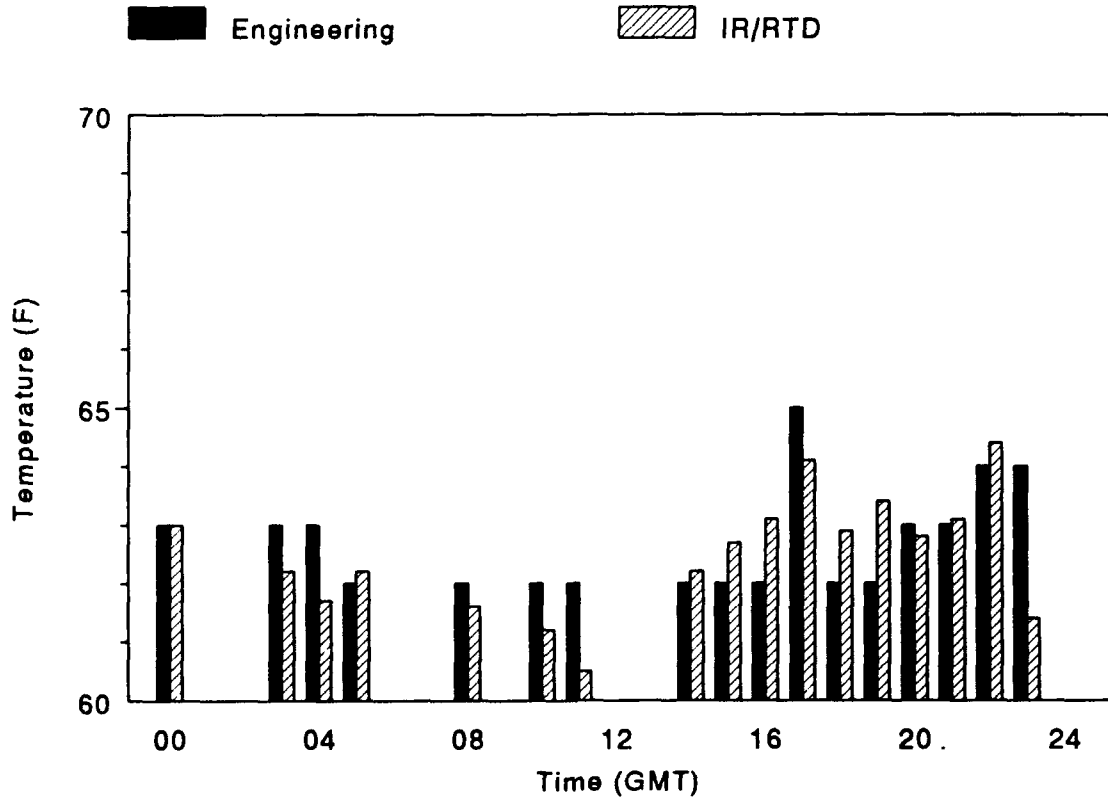
## Air Temperature

July 21, 1991



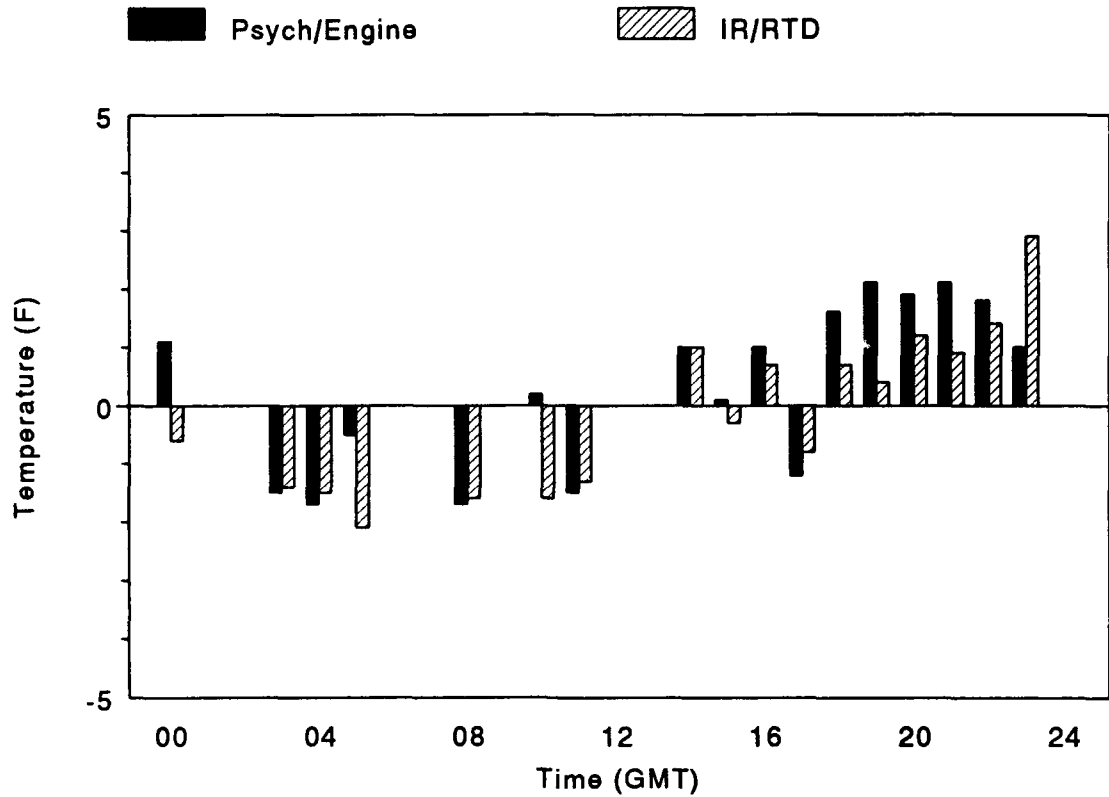
## Sea-surface Temperature

July 21, 1991



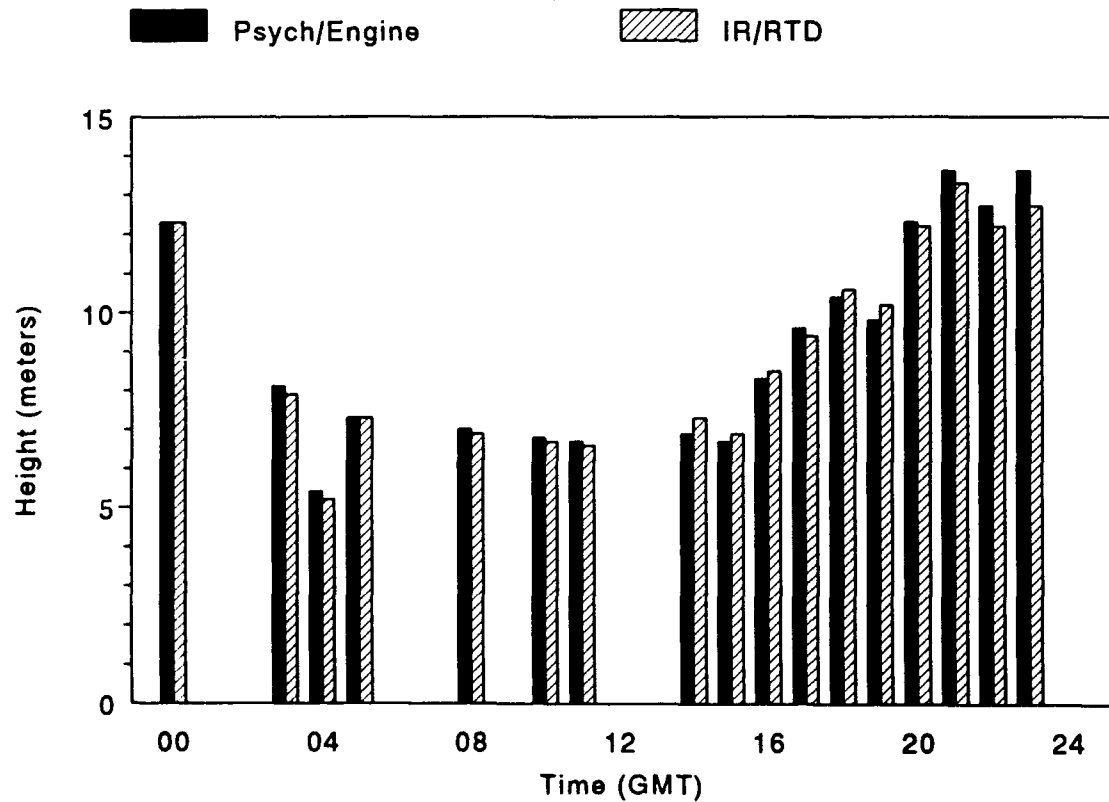
# Air/Sea-surface Temperature Difference

July 21, 1991



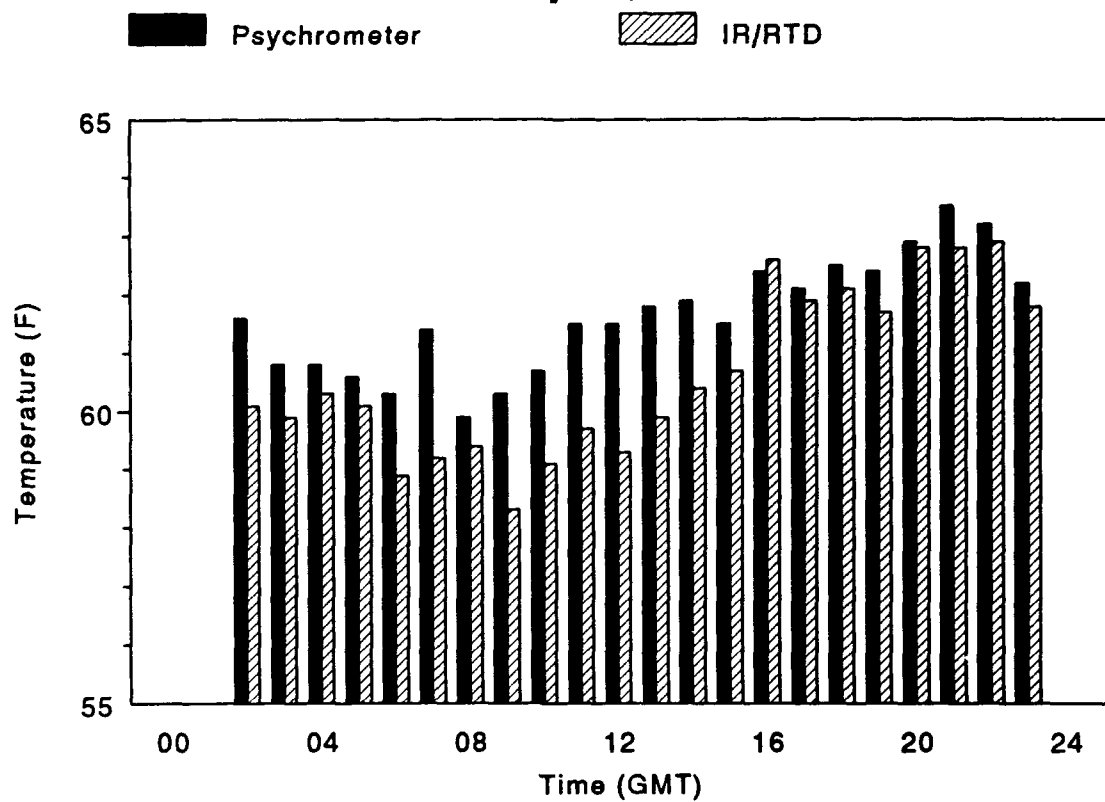
# Evaporation Duct Height

July 21, 1991



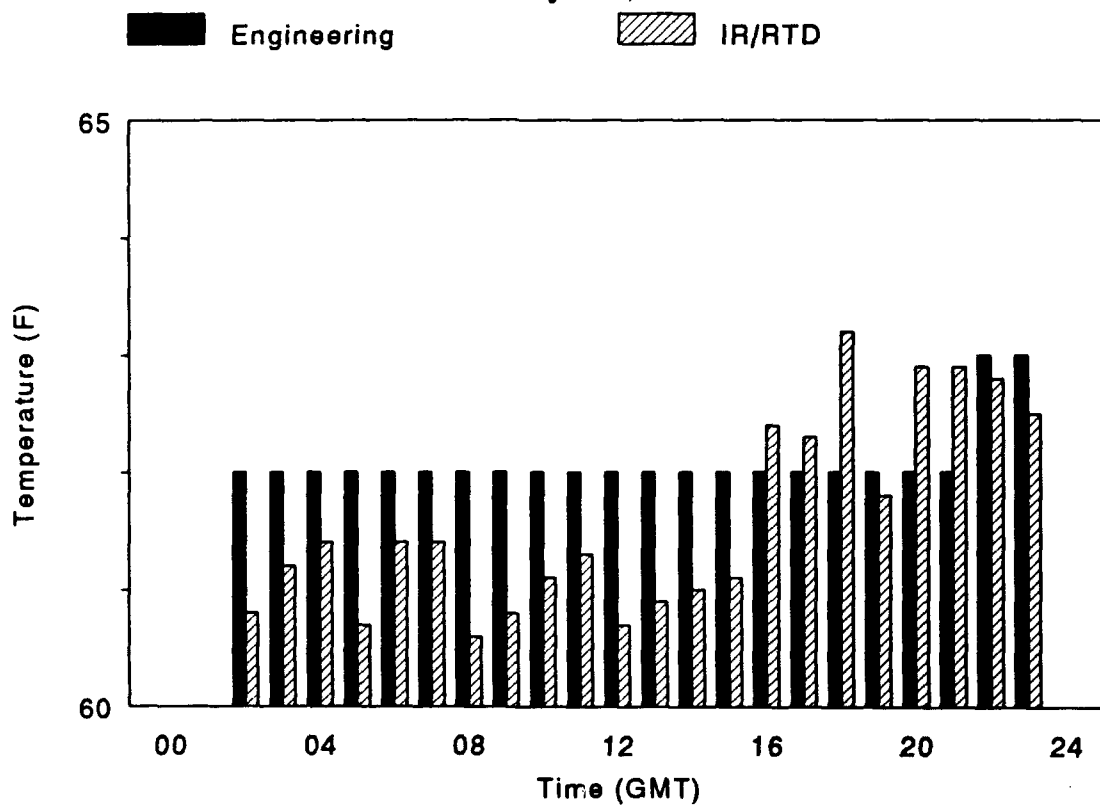
## Air Temperature

July 22, 1991



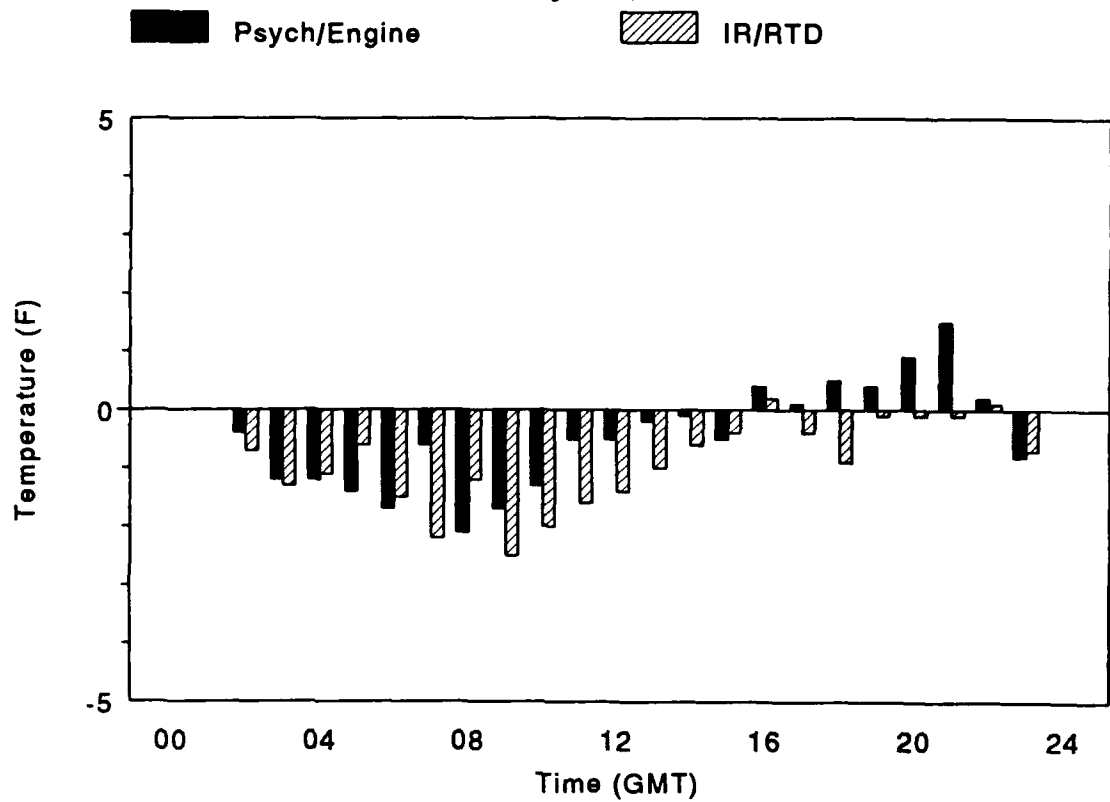
## Sea-surface Temperature

July 22, 1991



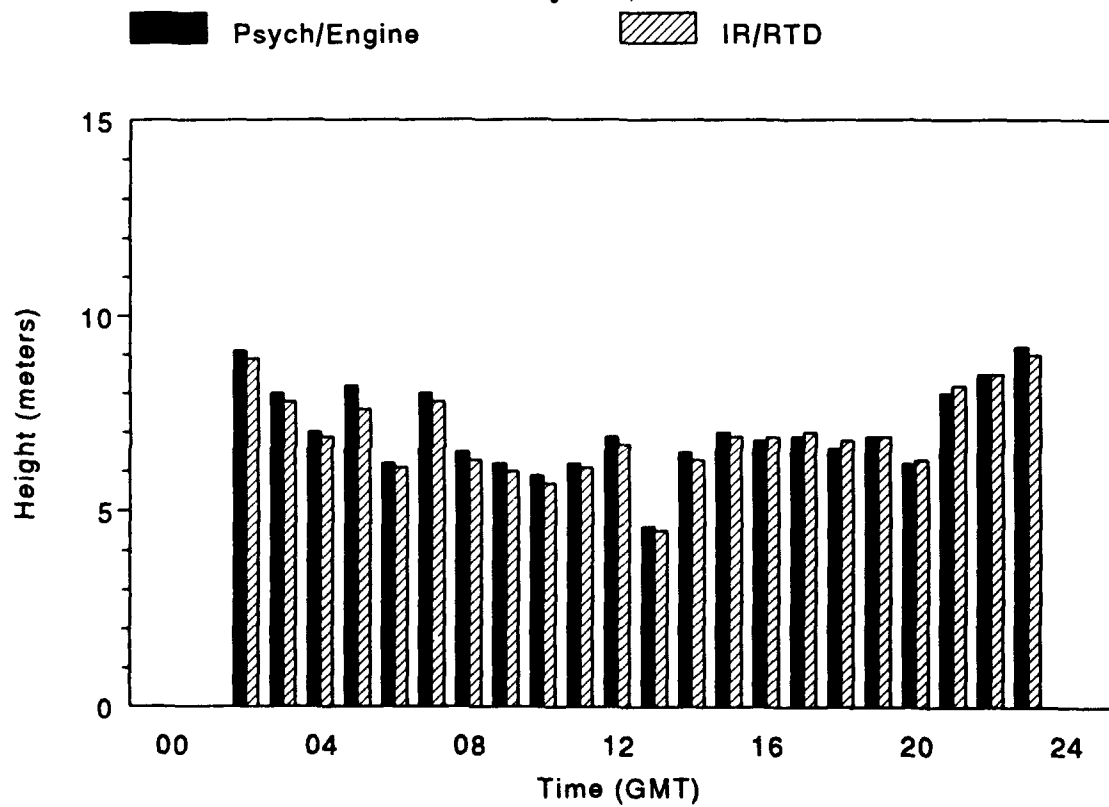
## Air/Sea-surface Temperature Difference

July 22, 1991



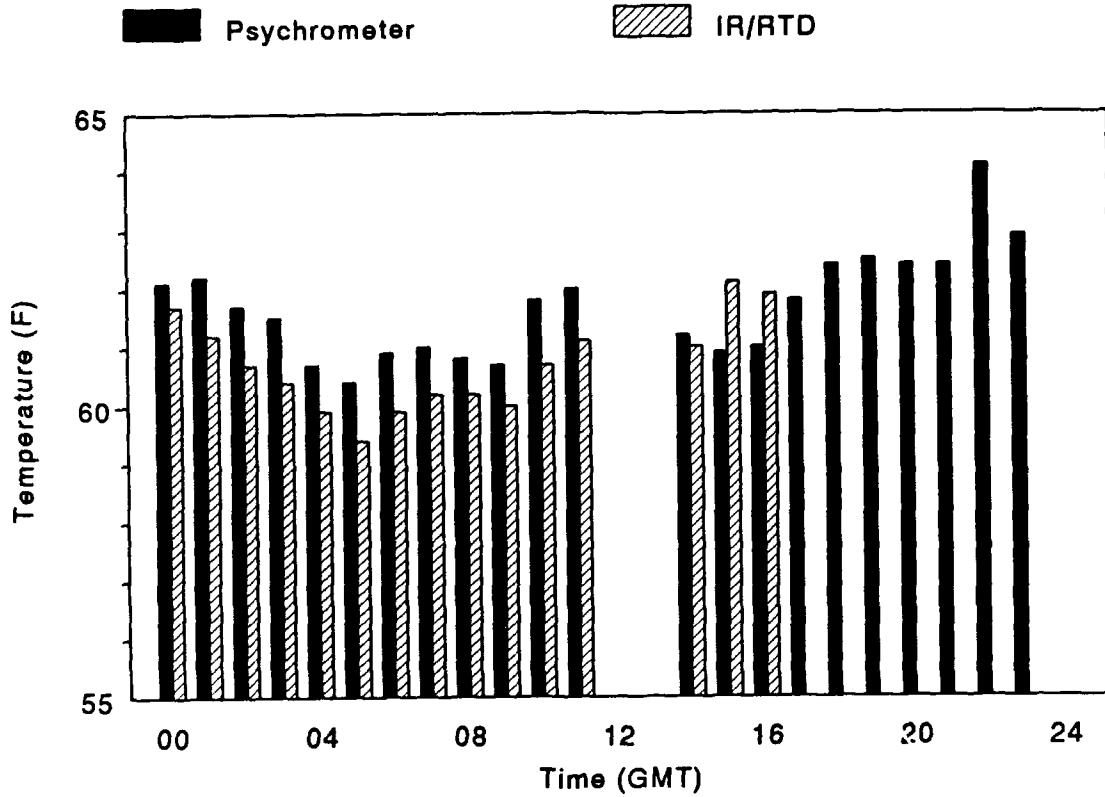
## Evaporation Duct Height

July 22, 1991



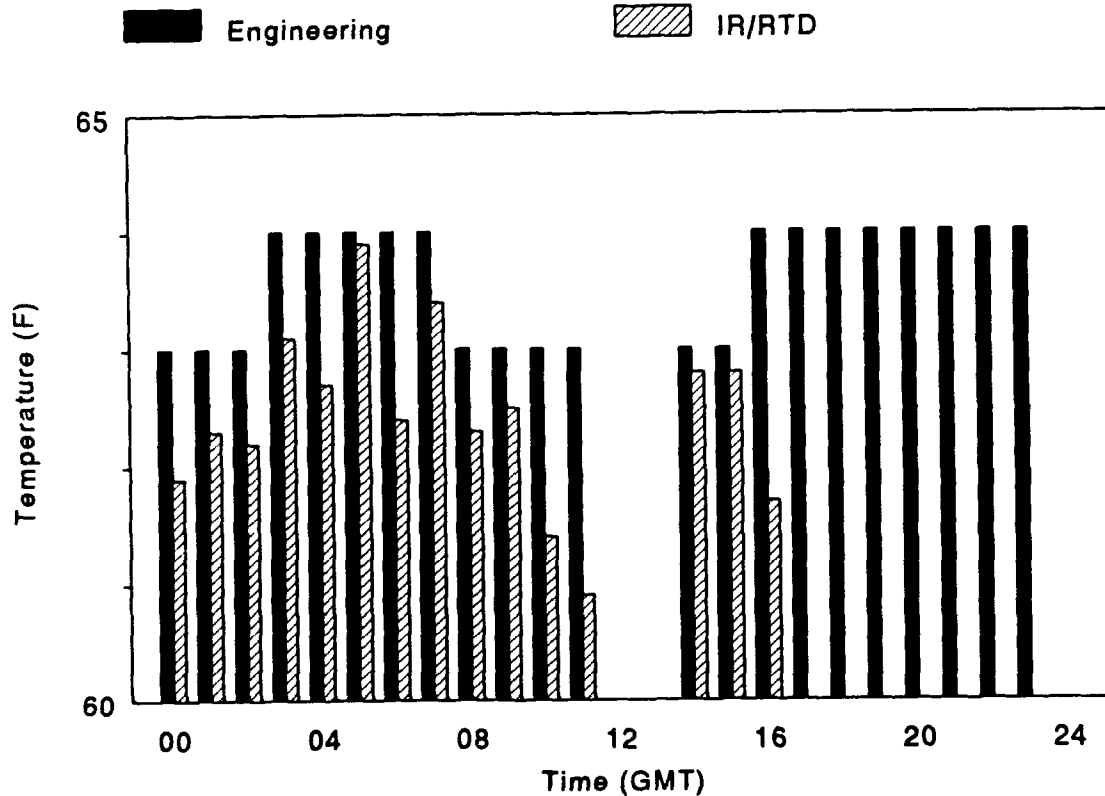
## Air Temperature

July 23, 1991



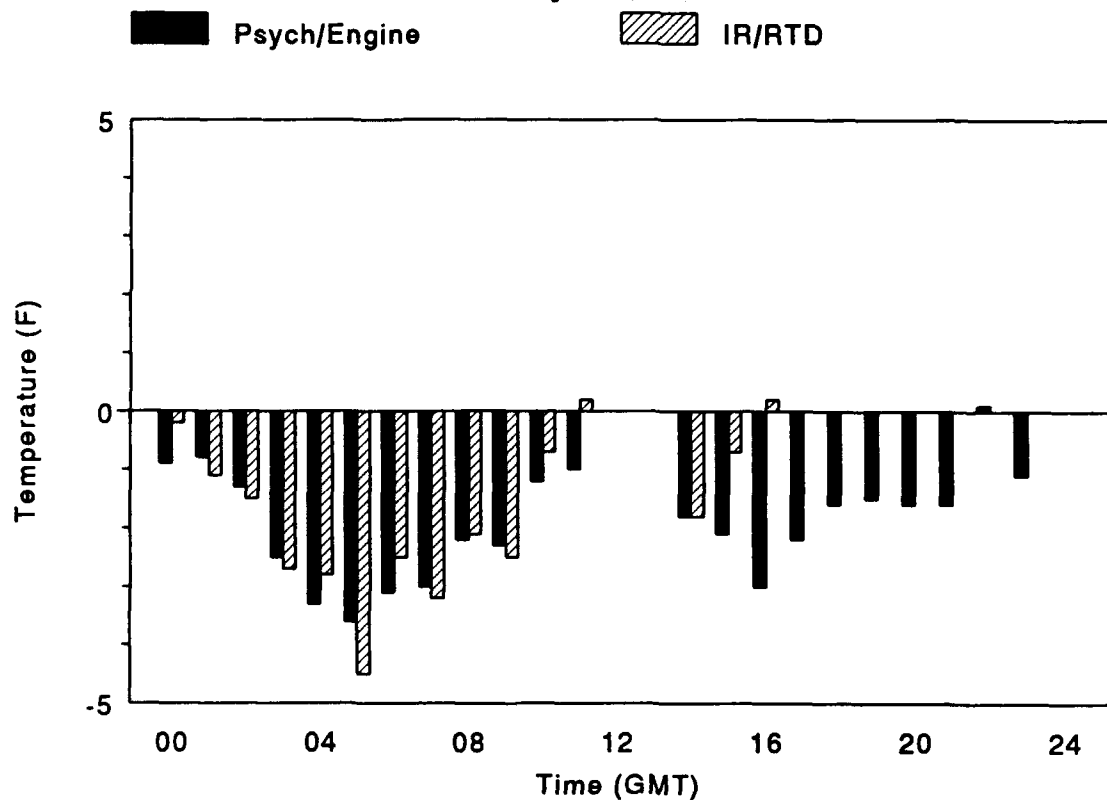
## Sea-surface Temperature

July 23, 1991



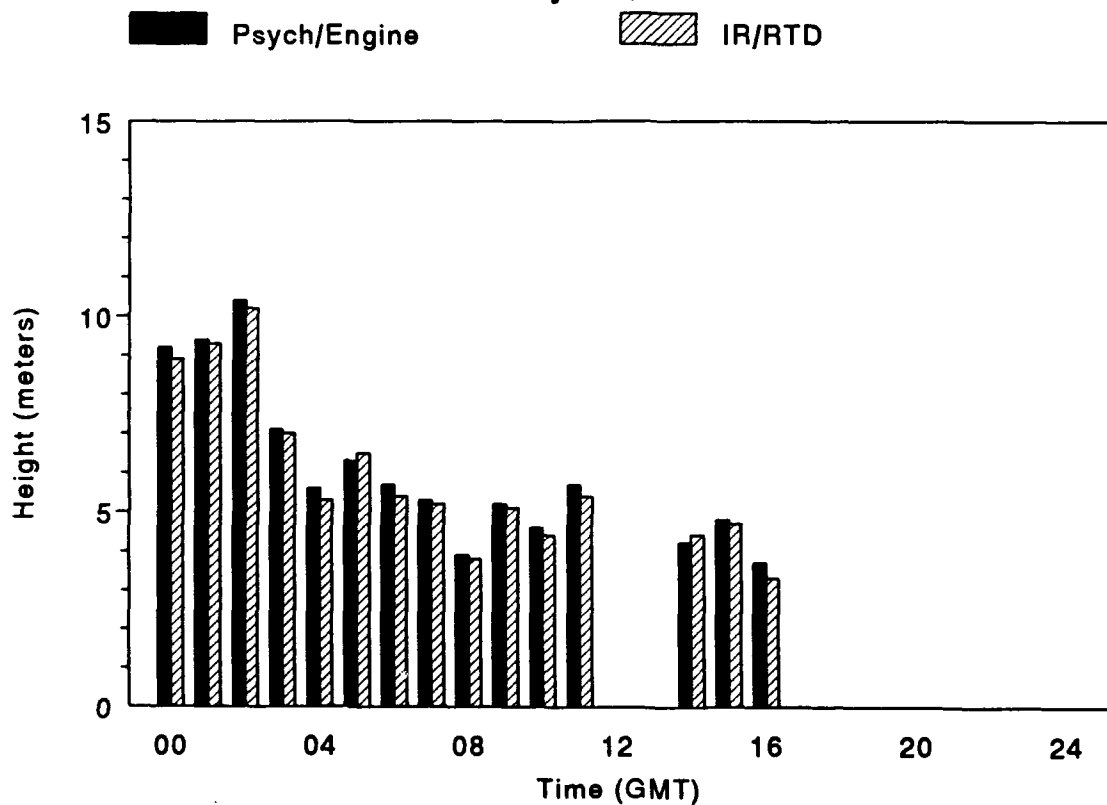
# Air/Sea-surface Temperature Difference

July 23, 1991



# Evaporation Duct Height

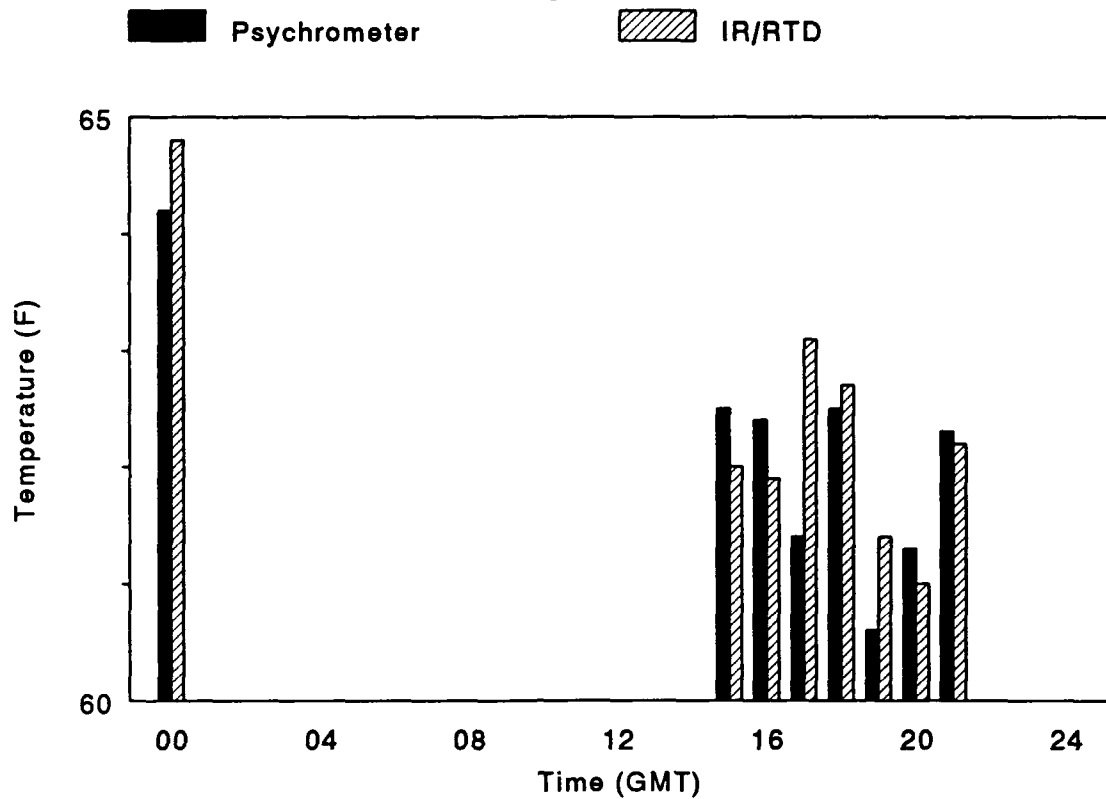
July 23, 1991





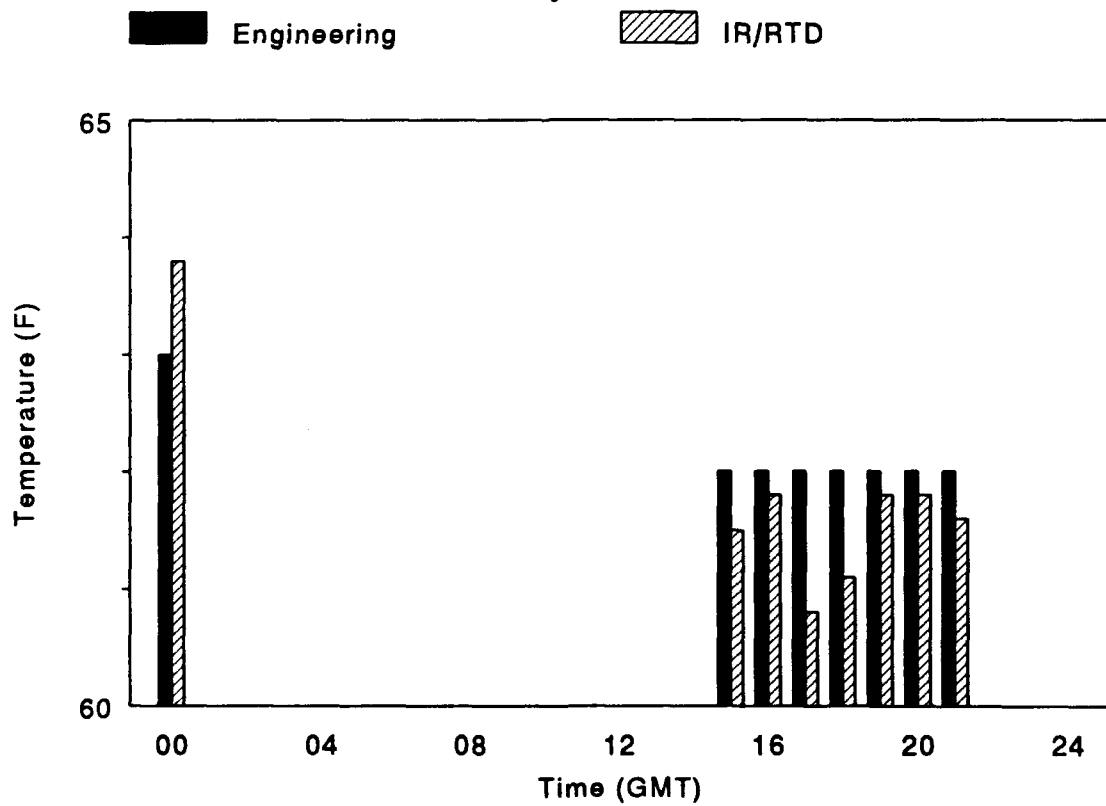
## Air Temperature

July 24, 1991



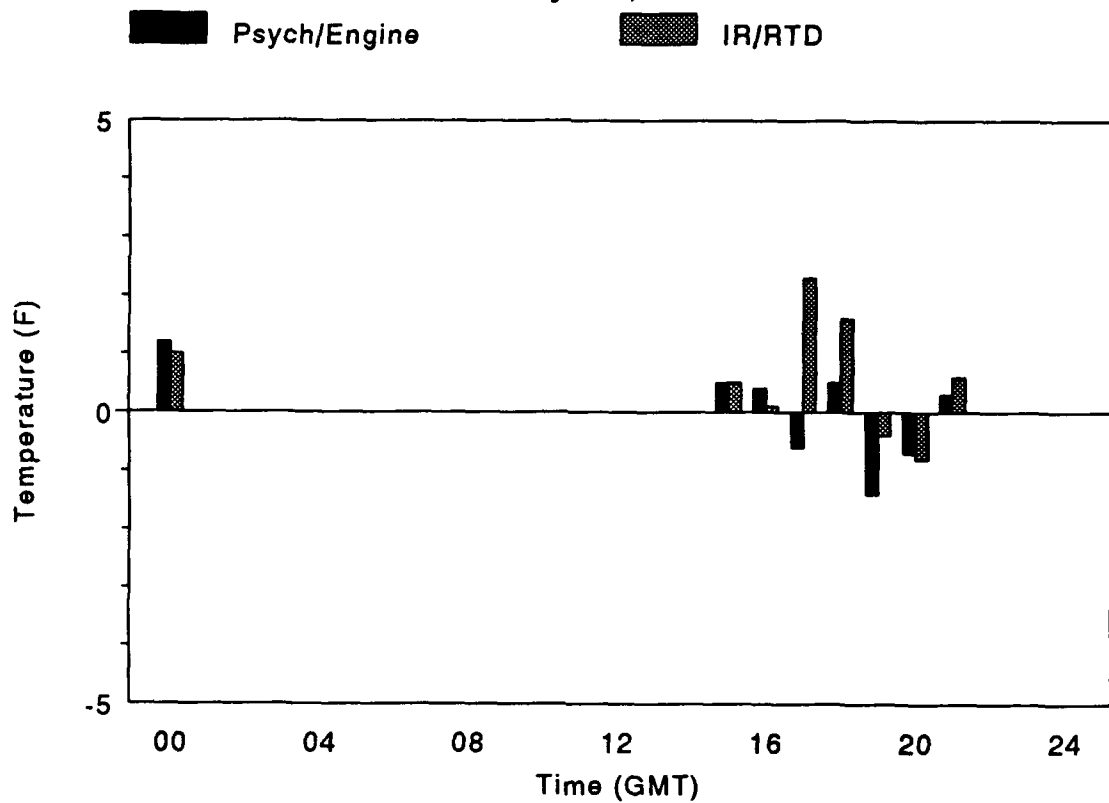
## Sea-surface Temperature

July 24, 1991



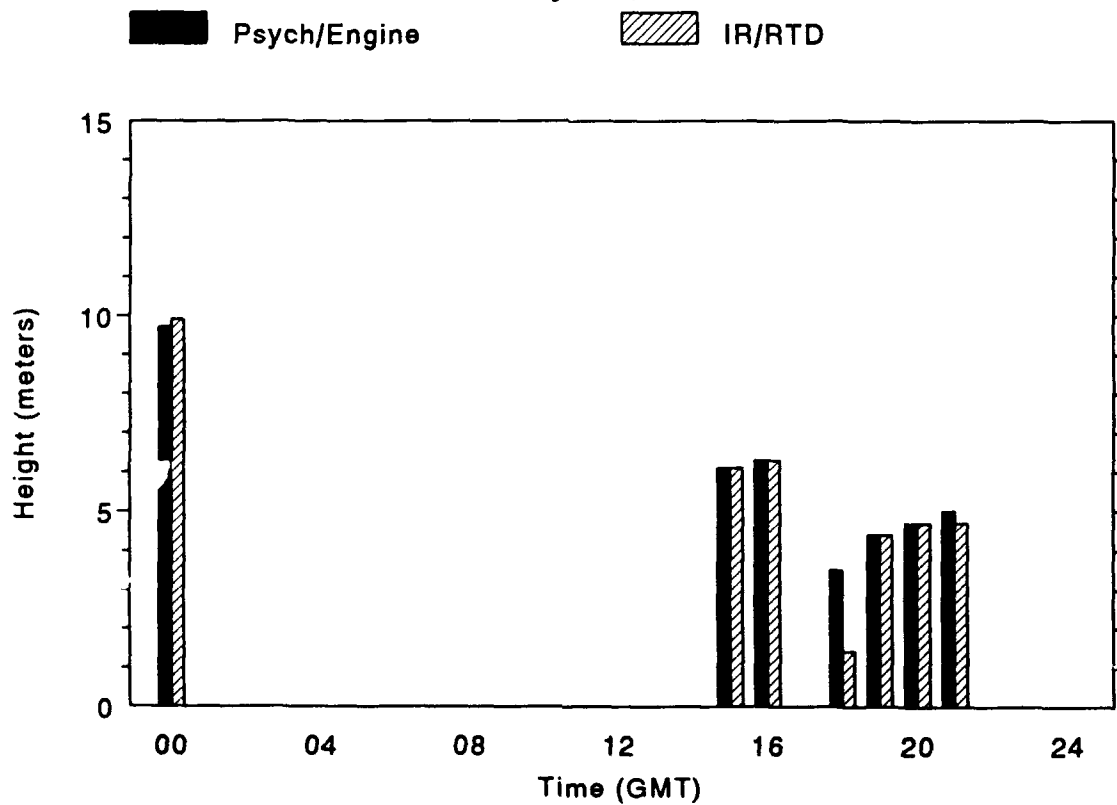
# Air/Sea-surface Temperature Difference

July 24, 1991



# Evaporation Duct Height

July 24, 1991



REPORT DOCUMENTATION PAGE			Form Approved OMB No. 0704-0188	
Public reporting burden for this collection of information is estimated to average 1 hour per response, including the time for reviewing instructions, searching existing data sources, gathering and maintaining the data needed, and completing and reviewing the collection of information. Send comments regarding this burden estimate or any other aspect of this collection of information, including suggestions for reducing this burden, to Washington Headquarters Services, Directorate for Information Operations and Reports, 1215 Jefferson Davis Highway, Suite 1204, Arlington, VA 22202-4302, and to the Office of Management and Budget, Paperwork Reduction Project (0704-0188), Washington, DC 20503.				
1. AGENCY USE ONLY (Leave blank)		2. REPORT DATE June 1992		3. REPORT TYPE AND DATES COVERED Final: Jun 91 — Oct 91
4. TITLE AND SUBTITLE AN EVALUATION OF AN INFRARED/RESISTANCE TEMPERATURE DEVICE FOR AIR/SEA-SURFACE TEMPERATURE MEASUREMENTS		5. FUNDING NUMBERS PE: 0603207N PROJ: X2008 SUBPROJ: 54-MP67-01 ACC: DN305062		
6. AUTHOR(S) W. L. Patterson		8. PERFORMING ORGANIZATION REPORT NUMBER NRaD TD 2271		
7. PERFORMING ORGANIZATION NAME(S) AND ADDRESS(ES) Naval Command, Control and Ocean Surveillance Center (NCCOSC) RDT&E Division (NRaD) San Diego, CA 92152-5000		10. SPONSORING/MONITORING AGENCY REPORT NUMBER		
9. SPONSORING/MONITORING AGENCY NAME(S) AND ADDRESS(ES) Space and Naval Warfare Systems Command (PMW-165) Washington, DC 20363-5100		11. SUPPLEMENTARY NOTES		
12a. DISTRIBUTION/AVAILABILITY STATEMENT  Approved for public release; distribution is unlimited.		12b. DISTRIBUTION CODE		
13. ABSTRACT (Maximum 200 words)  An infrared/resistance temperature device (IR/RTD) and a hand-held psychrometer were used at sea for 12 days, onboard the <i>USS Ranger</i> (CV 61), to gather air and sea-surface temperatures. Although not supported by the evaporation duct height calculations of this test period, the clearly artificial trend in sea-surface temperature readings reported from the seawater intake makes the IR/RTD the preferred instrument to measure sea-surface temperatures.  While tests reported in this document were primarily setup to see if the IR/RTD is practical for use in evaporation duct calculations, two other uses of the device were identified: (a) it was determined that sea-surface temperatures as an aid in forecasting the time fog will dissipate, and (b) it was used to sense the temperatures of sensitive electronic equipment, thus permitting operators to safely turn off their equipment when the maximum operating temperature was reached.				
14. SUBJECT TERMS evaporation ducts electromagnetic radiation infrared/resistance temperature device (IR/RTD) height duct			15. NUMBER OF PAGES 55	
			16. PRICE CODE	
17. SECURITY CLASSIFICATION OF REPORT UNCLASSIFIED	18. SECURITY CLASSIFICATION OF THIS PAGE UNCLASSIFIED	19. SECURITY CLASSIFICATION OF ABSTRACT UNCLASSIFIED	20. LIMITATION OF ABSTRACT SAME AS REPORT	

# INITIAL DISTRIBUTION

Code 0012	Patent Counsel	(1)
Code 0144	R. November	(1)
Code 144	V. Ware	(1)
Code 541	J. Olson	(1)
Code 543	W. L. Patterson	(25)
Code 961	Archive/Stock	(6)
Code 964B	Library	(2)

Defense Technical Information Center  
Alexandria, VA 22304-6145 (4)

NCCOSC Washington Liaison Office  
Washington, DC 20363-5100

Center for Naval Analyses  
Alexandria, VA 22302-0268

Navy Acquisition, Research & Development  
Information Center (NARDIC)  
Washington, DC 20360-5000

Space & Naval Warfare Systems Command  
Washington, DC 20363-5100 (2)

Naval Postgraduate School  
Monterey, CA 93943-5100